Natural Resources Canada | Ressources naturelles Canada

GEOLOGICAL SURVEY OF CANADA
OPEN FILE 9148

Till geochemical data for the Brazil Lake pegmatite area, southwest Nova Scotia (NTS 21-A/04, 20-O/16 and 20-P/13): samples collected in 2020, 2021, and 2022

D.M. Brushett, C.E. Beckett-Brown, M.B. McClenaghan, R.C. Paulen, J.M. Rice, A. Haji Egeh, and P. Pelchat

2024

Canada

GEOLOGICAL SURVEY OF CANADA
OPEN FILE 9148

Till geochemical data for the Brazil Lake pegmatite area, southwest Nova Scotia (NTS 21-A/04, 20-O/16 and 20-P/13): samples collected in 2020, 2021, and 2022

D.M. Brushett[1], C.E. Beckett-Brown[2], M.B. McClenaghan[3], R.C. Paulen[3], J.M. Rice[3], A. Haji Egeh[3], and P. Pelchat[3]

[1]Nova Scotia Department of Natural Resources and Renewables, 1701 Hollis Street, Halifax, Nova Scotia
[2]Ontario Geological Survey, 933 Ramsey Lake Road, Sudbury, Ontario
[3]Geological Survey of Canada, 601 Booth Street, Ottawa, Ontario

2024

Permanent link: https://doi.org/10.4095/332384

This publication is available for free download through GEOSCAN (https://geoscan.nrcan.gc.ca/).

Recommended citation

Brushett, D.M., Beckett-Brown, C.E., McClenaghan, M.B., Paulen, R.C., Rice, J.M., Haji Egeh, A., and Pelchat, P., 2024. Till geochemical data for the Brazil Lake pegmatite area, southwest Nova Scotia (NTS 21-A/04, 20-O/16 and 20-P/13): samples collected in 2020, 2021, and 2022; Geological Survey of Canada, Open File 9148, 1 .zip file. https://doi.org/10.4095/332384

Publications in this series have not been edited; they are released as submitted by the author.

ISSN 2816-7155
ISBN 978-0-660-69371-2
Catalogue No. M183-2/9148E-PDF

TABLE OF CONTENTS

Abstract 1

Introduction 1

Location and access 2

Geology 4

- Bedrock geological setting 4
- Local bedrock geology and mineralization 4
- Deposit discovery 5
- Surficial geology 5
- Till characteristics 7

Previous surficial geochemical and mineralogical studies 10

Methods 10

- Till sampling 11
- Sample processing 12
- Geochemical analysis 12

Results 15

- Till geochemistry 15
- Till geochemistry spatial patterns 23

Discussion 26

- Size fraction comparison 26
- Comparison of Na-peroxide fusion and aqua regia digestion 27
- Comparison of Na-peroxide fusion and 4-acid digestion 27
- Brazil Lake dispersal train 29
- Comparison to other studies 29
- Future work 29

Conclusions and recommendations for exploration 31

- What is the optimal digestion method and size fraction of till for Li exploration? 31
- What is the optimal sample spacing/density and survey orientation? 32

Acknowledgements 32

References 32

Figures

- Figure 1. Bedrock geology of southwestern Nova Scotia 2
- Figure 2. a) Bedrock geology of the Brazil Lake study area superimposed on a LiDAR hillshade image showing the location of till samples collected in 2020, 2021, and 2022 and mineral occurrences. The direction and relative age of ice-flow phases are also shown. b) Close-up of the location of till samples around the Brazil Lake and Army Road pegmatites. 3
- Figure 3. Photographs of a) coarse-grained white spodumene crystals exposed on the weathered subcropping surface of the South pegmatite; b) a fresh unweathered spodumene boulder extracted from the South pegmatite; c) tantalite crystals in quartz at the North pegmatite; d) cross-section of the South pegmatite in contact with the metavolcanic country rocks. At the outer contact of the pegmatite, abundant tourmaline is observed, which formed as a result of the exsolution of boron- rich fluids from the pegmatite. 5
- Figure 4. Photograph showing abundant spodumene-bearing float boulders that are exposed on the surface south and east of the North Pegmatite. 5
- Figure 5. Map showing the generalized ice-flow chronology of southern Nova Scotia. 6

Figure 6. Photographs of subglacial traction (lodgement) till sampled at various sites in the Brazil Lake study area. a) Site 22MPB026 after sampling. b) Site 22MPB036. Note the overconsolidated chunks of till on the shovel and the white spodumene clast. c) Site 22MPB027 after sampling showing well developed A, B, and C soil horizons. d) Site 22MPB027 showing an overconsolidated chunk of till on the shovel. e) Site 22MPB-038 after sampling showing subhorizontal fissility behind the shovel. 7
Figure 7. Photograph of spodumene clasts from the pegmatites, which were readily visible while sampling tills in backhoe trenches just down-ice of the pegmatites. 7
Figure 8. Photograph of the striated bedrock surface that was exposed from previous stripping of the South pegmatite. 8
Figure 9. Photographs of a) subglacial melt out till that was observed as a thin (<2 m) horizon containing well sorted lenses and layers of sand in a coastal section (Beaver River till type locality); b) upper melt-out till observed in a quarry section showing loose, sorted sandy lenses and beds. Clasts and boulders from this horizon are generally composed of locally derived angular greywacke boulders; c) a thin upper melt-out till horizon, which was only identified on the southeastern flank of a drumlin from the Salmon River coastal section; and d) a close-up view of the upper melt-out till facies from Salmon River costal section showing pale sandy till with abundant local, mostly angular clast lithologies. 8
Figure 10. a) Photograph of the of subglacial melt-out till sampled at site 22MPB023. Subglacial melt-out till is typically looser than subglacial traction till and also contains lenses of sorted sand (b and c) within the till. 9
Figure 11. Ternary diagram showing the percentage of sand, silt, and clay in till matrix of the till samples. 9
Figure 12. Location of GSC till samples collected in 2022 in backhoe trenches excavated proximal to the North and South pegmatites. Pegmatite subcrops exposed by previous stripping are outlined and the regional ice-flow directions are indicated. 10
Figure 13. Photographs of a) the Salmon River sand unit showing the location of an optical stimulated luminescence (OSL) dating sample site; b) the Salmon River sand unit, which is the location of an OSL dating sample site, showing how the sand unit transitions upwards from a lower, grey, well sorted, fine-grained sand facies with abundant shells and shell fragments to a beige to orange-brown, medium-grained sandy facies with fewer shell fragments; c) several larger intact shells, which were collected for dating and identification. .11
Figure 14. Proportional dot maps of Li concentrations in till: a) the <0.063 mm till fraction analyzed using Na-peroxide fusion followed by ICP-MS; b) the 1.0–2.0 mm till fraction analyzed using Na-peroxide fusion followed by ICP-MS; c) the <0.063 mm till fraction analyzed using 4-acid digestion followed by ICP-MS; d) the 1.0–2.0 mm till fraction analyzed using 4-acid digestion followed by ICP-MS; e) the <0.063 mm till fraction analyzed using aqua regia digestion followed by ICP-MS; and f) the 1.0–2.0 mm till fraction analyzed using aqua regia digestion followed by ICP-MS. 17
Figure 15. Scatter plots comparing the three digestion methods to their size fraction counterparts (samples from 2020–2022). Concentrations of Li in <0.063 mm fraction determined by Na-peroxide fusion versus Li concentrations determined by (a) aqua regia and by (b) 4-acid. Concentrations of Li (ppm) in the 1.0–2.0 mm fraction determined by Na-peroxide fusion versus Li concentrations determined by (c) aqua regia and by (d) 4-acid. . . .23
Figure 16. Scatter plots comparing the concentrations of Li in the 1–2 mm fraction and the <0.063 mm fraction determined by (a) aqua regia, (b) 4-acid, and (c) Na-peroxide fusion for samples collected in 2020 through 2022. 24
Figure 17. Scatter plots comparing the concentrations of a) Ti, b) Zn, c) Sr, d) Sn, and e) Th determined by Na-peroxide fusion and pXRF for the <0.063 mm and 1.0–2.0 mm fractions .25
Figure 18. Proportional dot maps illustrating the difference between Li concentrations in the 1.0–2.0 mm and the <0.063 mm fractions analyzed by Na-peroxide fusion. 28

Tables

Table 1. Summary of analytical methods, size fractions, analytical lab report numbers and the location of data reported in appendices. 13

Table 2. The lower and upper detection limits for the <0.002 mm, <0.063 mm (silt + clay), and 1.0–2.0 mm (coarse) sized fractions of till for samples collected in 2020, 2021, and 2022. 14

Table 3. Comparison of Li concentrations in till samples collected up-ice and down-ice of the North and South pegmatites. 15

Table 4. Summary statistics for lithium-cesium-tantalum (LCT) pegmatite pathfinder elements in the <0.063 mm and the 1.0–2.0 mm till fractions. 16

Table 5. Comparison of lithium statistics for the three digestion methods and two size fractions used in this study. 27

Table 6. Cost comparison for aqua regia, Na-peroxide fusion and 4-acid digestion methods for the <0.063 mm and 1.0–2.0 mm fractions. 29

Table 7. Listing of pathfinder elements that display anomalous concentrations around the Brazil Lake pegmatites, the Army Road pegmatite, and other locations in the study area 30

Table 8. Lithium concentrations reported for other till geochemical studies and surveys compared to the concentrations reported in this study. 30

Appendices

Appendix A

Appendix A1. Metadata for 2020, 2021, and 2022 till samples.

Appendix A2. Descriptions of analytical methods used by Bureau Veritas Mineral Laboratories Canada.

Appendix A3. Descriptions of analytical methods used by SGS Canada Inc.

Appendix B

Appendix B1. Field observations, location data, lab sample numbers, quality assurance/ quality control (QA-QC) sample data, Munsell colour, and matrix grain-size data.

Appendix B2. Photographs of the sites where samples were collected in 2021 and 2022 (21DB, 22DB, and 22MPB series samples).

Appendix B3a. Map showing the locations of the till samples used in this study.

Appendix B3b. Close-up location map of till sample sites around the North and South Brazil Lake pegmatites and the Army Road pegmatite.

Appendix B4. Bedrock geology legend for Appendix B3.

Appendix C. Unedited (raw) geochemical data reported by the laboratories and laboratory certifications. Refer to Table 1 for a summary list of files and explanations.

BBM22-15771.pdf Lab certificate and Na-peroxide fusion data for the <0.063 mm fraction of the 21DB series samples: data listing and lab certificate.

BBM22-15771.xlsx Na-peroxide fusion data for the <0.063 mm fraction of the 21DB series samples.

BBM22-15938.pdf Lab certificate and Na-peroxide fusion data for the 1.0–2.0 mm fraction of the 21DB series samples: data listing and lab certificate.

BBM22-15938.xlsx Na-peroxide fusion data for the 1.0–2.0 mm fraction of the 21DB series samples.

BBM23-25458.pdf Lab certificate and Na-peroxide fusion data for the <0.063 mm fraction of the 22DB and 22MPB series samples: data listing and lab certificate.

BBM23-25458.xlsx Na-peroxide fusion data for the <0.063 mm fraction of the 22DB and 22MPB series samples.

BBM23-25716.pdf Lab certificate and Na-peroxide fusion data for the 1.0–2.0 mm fraction of the 22MPB series samples.

BBM23-25716.xls Na-peroxide fusion data for the 1.0–2.0 mm fraction of the 22MPB series samples.

VAN21000506.pdf Lab certificate and Aqua regia, 4-acid digestion, and Li-metaborate fusion data for the <0.063 mm fraction of 20DB series: data listing and lab certificate.

VAN21000506.xlsx Aqua regia and 4-acid digestion, and Li-metaborate fusion data for the <0.063 mm fraction of 20DB series samples.

VAN21000507.pdf Lab certificate and Aqua regia, 4-acid digestion, and Li-metaborate fusion data for the 1.0–2.0 mm fraction of 20DB series samples: data listing and lab certificate.

VAN21000507.xlsx Aqua regia, 4-acid digestion, and Li-metaborate fusion data for the 1.0–2.0 mm fraction of 20DB series samples.

VAN21000508.pdf Lab certificate and Aqua regia, 4-acid digestion, and Li-metaborate fusion data for the <0.002 mm fraction of 20DB series: data listing and lab certificate.

VAN21000508.xlsx Aqua regia, 4-acid digestion, and Li-metaborate fusion data for the <0.002 mm fraction of 20DB series samples.

VAN23000186.pdf Lab certificate and Aqua regia data for the <0.063 and 1.0–2.0 mm fraction of the 21DB and 22MPB series samples: data listing and lab certificate.

VAN23000186.xlsx Aqua regia data for the <0.063 mm and 1.0–2.0 mm fraction of the 21DB and 22MPB series samples.

VAN23000187.pdf Lab certificate and Aqua regia and 4-acid digestion data for the <0.063 mm fraction of the 22DB and 22MPB series samples: data listing and lab certificate.

VAN23000187.xlsx Aqua regia data for the <0.063 mm fraction of the 22DB and 22MPB series samples.

VAN23000250.pdf Lab certificate and Aqua regia data for the 1.0–2.0 mm fraction of the 22MPB series samples: data listing and lab certificate.

VAN23000250.xlsx Aqua regia data for the 1.0–2.0 mm fraction of the 22MPB series samples.

VAN23000852_2.pdf Lab certificate and 4-acid digestion data for the <0.063 and 1.0–2.0 mm fraction of the 22MPB series samples: data listing and lab certificate.

VAN23000852_2.xlsx 4-acid digestion data for the <0.063 mm and 1.0–2.0 mm fraction of the 22MPB series samples.

VAN23001111.pdf Lab certificate and 4-acid digestion reanalysis data for the <0.063 mm fraction of a subset of the 22MPB series samples: data listing and lab certificate.

VAN23001111.xlsx 4-acid digestion reanalysis data for the <0.063 mm fraction of a subset of the 22MPB series samples.

GSC_Till-pH.xlsx pH values for selected till samples.

Appendix D. Formatted geochemical data listings

Appendix D1. Aqua regia data for the <0.002, <0.063, and 1.0–2.0 mm fractions of 20DB, 21DB, 22DB, and 22MPB series samples.

Appendix D2. 4-acid data for the <0.002, <0.063, and 1.0–2.0 mm fractions of 20DB and 22DB series samples and the <0.063 and 1.0–2.0 mm fractions of 22MPB series samples.

Appendix D3. Na-peroxide fusion data for the <0.063 and 1.0–2.0 mm fractions of 21DB, 22DB and 22MPB series samples.

Appendix D4. Li metaborate fusion data for the <0.002, <0.063, and 1.0–2.0 mm fractions of 2020-DB series samples.

Appendix D5. Combined master geochemical data used for GIS plotting.

Appendix D6. Comparison of Li (ppm) concentrations in the <0.063 and 1–2 mm fractions for aqua regia and Na-peroxide fusion and the ratio between the values reported for each analytical method.

Appendix E. pXRF data for the <0.063 and 1.0–2.0 mm fraction of 22MPB series samples

Appendix E1. Raw pXRF data.

Appendix E2. Comparison of pXRF data and Na-peroxide fusion data for Ti, Zn, Sr, Sn, and Th.

Appendix F. Log transformed data correlation matrices for all of the digestion methods and size fractions.

Appendix G. Till geochemistry proportional dot maps of selected geochemical data for the <0.063 and 1.0–2.0 mm size fractions of till plotted on a bedrock geology base (White et al., 2012) superimposed on a LiDAR hillshade image (azimuth of 315°). The bedrock geology legend is shown in Figure 2.

Map 1. Proportional dot maps of Cs concentrations for the <0.063 mm till fraction analyzed using Na-peroxide fusion followed by ICP-MS (n=152).

Map 2. Proportional dot maps of Cs concentrations for the 1.0–2.0 mm till fraction analyzed using Na-peroxide fusion followed by ICP-MS (n=104).

Map 3. Proportional dot maps of Cs concentrations for the <0.063 mm till fraction analyzed using 4-acid digestion followed by ICP-MS (n=91).

Map 4. Proportional dot maps of Cs concentrations for the 1.0–2.0 mm till fraction analyzed using 4-acid digestion followed by ICP-MS (n=29).

Map 5. Proportional dot maps of Ta concentrations for the <0.063 mm till fraction analyzed using Na-peroxide fusion followed by ICP-MS (n=152).

Map 6. Proportional dot maps of Ta concentrations for the 1.0–2.0 mm till fraction analyzed using Na-peroxide fusion followed by ICP-MS (n=104).

Map 7. Proportional dot maps of Ta concentrations for the <0.063 mm till fraction analyzed using 4-acid digestion followed by ICP-MS (n=91).

Map 8. Proportional dot maps of Ta concentrations for the 1.0–2.0 mm till fraction analyzed using 4-acid digestion followed by ICP-MS (n=29).

Map 9. Proportional dot maps of Be concentrations for the 1.0–2.0 mm till fraction analyzed using Na-peroxide fusion digestion followed by ICP-MS (n=104).

Map 10. Proportional dot maps of Rb concentrations for the <0.063 mm till fraction analyzed using Na-peroxide fusion followed by ICP-MS (n=152).

Map 11. Proportional dot maps of Rb concentrations for the 1.0–2.0 mm till fraction analyzed using Na-peroxide fusion followed by ICP-MS (n=104).

Map 12. Proportional dot maps of Rb concentrations for the <0.063 mm till fraction analyzed using 4-acid digestion followed by ICP-MS (n=91).

Map 13. Proportional dot maps of Rb concentrations for the 1.0–2.0 mm till fraction analyzed using 4-acid digestion followed by ICP-MS (n=29).

Map 14. Proportional dot maps of Zr concentrations for the <0.063 mm till fraction analyzed using 4-acid digestion followed by ICP-MS (n=91).

Map 15. Proportional dot maps of Nb concentrations for the <0.063 mm till fraction analyzed using Na-peroxide fusion followed by ICP-MS (n=91).

Map 16. Proportional dot maps of Nb concentrations for the 1.0–2.0 mm till fraction analyzed using Na-peroxide fusion followed by ICP-MS (n=104).

Map 17. Proportional dot maps of Nb concentrations for the <0.063 mm till fraction analyzed using 4-acid digestion followed by ICP-MS (n=91).

Map 18. Proportional dot maps of Nb concentrations for the 1.0–2.0 mm till fraction analyzed using 4-acid digestion followed by ICP-MS (n=29).

Map 19. Proportional dot maps of Sn concentrations for the <0.063 mm till fraction analyzed using 4-acid digestion followed by ICP-MS (n=91).

Map 20. Proportional dot maps of Sn concentrations for the 1.0–2.0 mm till fraction analyzed using 4-acid digestion followed by ICP-MS (n=29).

Map 21. Proportional dot maps of W concentrations for the <0.063 mm till fraction analyzed using 4-acid digestion followed by ICP-MS (n=91).

Map 22. Proportional dot maps of W concentrations for the 1.0–2.0 mm till fraction analyzed using 4-acid digestion followed by ICP-MS (n=29).

Appendix H. Quality Assurance/Quality Control (QA/QC) compilation and summary

Till geochemical data for the Brazil Lake pegmatite area, southwest Nova Scotia (NTS 21A/04, 20-O/16 and 20P/13): samples collected in 2020, 2021, and 2022

D.M. Brushett[1], C.E. Beckett-Brown[2], M.B. McClenaghan[3], R.C. Paulen[3], J.M. Rice[3], A. Haji Egeh[3], and P. Pelchat[3]

[1]Nova Scotia Department of Natural Resources and Renewables, 1701 Hollis Street, Halifax, NS B3J 3M8
[2]Ontario Geological Survey, 933 Ramsey Lake Road, Sudbury, ON P3E 6B5
[3]Geological Survey of Canada, 601 Booth Street, Ottawa, ON K1A 0E8

ABSTRACT

This open file reports geochemical data for till samples collected as a part of a till geochemical and surficial mapping project around the Brazil Lake lithium-cesium-tantalum (LCT-type) pegmatites in southwestern Nova Scotia (NTS map sheets 21A/04, 20-O/16, and 20P/13). To meet the increasing global demand for lithium and associated minerals (i.e. Cs, Ta, Be, In, Sn, and W), the Geological Survey of Canada (GSC) is investigating geochemical methods for exploration of these critical minerals. These types of deposits are important sources of Li, Sn, and Rb as well as the primary source of Ta. The research presented here is part of the GSC's Targeted Geoscience Initiative Program and has been carried out in partnership with the Nova Scotia Department of Natural Resources and Renewables (NSDNRR). The goal of the research is to increase exploration success in regions covered by glacial sediments by documenting how critical minerals and associated elements are glacially dispersed in till from pegmatites using the Brazil Lake property as a test area. Newly available light detection and radar (LiDAR) data assisted in deciphering ice-flow trajectories, which in turn, allowed for targeted till sampling. A total of 184 till samples were collected for geochemical analysis in 2020, 2021, and 2022 and the data reported here include widely spaced regional samples collected across southwest Nova Scotia, and proximal samples collected up- and down-ice of the Brazil Lake pegmatites. The widely spaced till samples provide the regional context for the interpretation of the closely spaced samples and aid in assessing the potential for additional pegmatites buried by extensive till cover. Data reported in this Open File include sample descriptions, locations, site photos, and geochemical analyses of the coarse sand (1.0–2.0 mm) and silt + clay (<0.063 mm) fractions of the till samples. For the 2020 samples only, the <0.002 mm (clay) fraction was also analyzed. Analyses completed over the 3 years (2020, 2021 2022) used varying combinations of digestion and fusion methods to test and compare their efficacy for the various pathfinder elements for LCT pegmatites: 1) aqua regia (partial) digestion, 2) Na-peroxide fusion (total), 3) 4-acid (near total) digestion, and 4) Li-meta/tetraborate fusion.

INTRODUCTION

In 2021 and 2022, the Geological Survey of Canada (GSC), in partnership with the Nova Scotia Department of Natural Resources and Renewables (NSDNRR), collected till samples around the Brazil Lake lithium-cesium-tantalum (LCT) pegmatite deposit in southwest Nova Scotia (Fig. 1; McClenaghan et al., 2023a, b; Brushett et al., 2023). This fieldwork was carried out as part of the critical mineral exploration research funded by the GSC's Targeted Geoscience Initiative (TGI) program. TGI is a national, collaborative, multidisciplinary geoscience research program to improve mineral exploration effectiveness. Developing next-generation geological models and knowledge, as well as cutting-edge tools and methods, will increase the understanding of the processes that formed Canada's mineral deposits and aid in identifying and developing novel indicators and parameters to guide exploration in emerging as well as existing mining areas (https://natural-resources.canada.ca/earth-sciences/earth-sciences-resources/targeted-geoscience-initiative-tgi/10907).

Although there have been many advancements in the use of till geochemistry to explore for a broad range of commodities (e.g. Au, Ag, Pt, Pd, Cu, Pb, Zn, U, W, Sn; McClenaghan and Paulen, 2018, and references therein), only a few case studies have tested till geochemical methods for discovering lithium-bearing pegmatites (e.g. Nikarinnen and Björklund, 1975; Steiger, 1977; Toverud, 1987; Ahtola et al. 2015). To address this knowledge gap, a detailed glacial sediment and bedrock study has been conducted around the Brazil Lake pegmatite deposit to (1) investigate how spodumene, the key ore mineral in the Brazil Lake deposit, was glacially dispersed in till and how it breaks down during glacial transport; (2) determine the geochemical signature of till from this style of mineralization; (3) define glacial dispersal patterns of the Li pegmatites; and (4) define the appropriate sampling protocols and analytical techniques that can be used for lithium

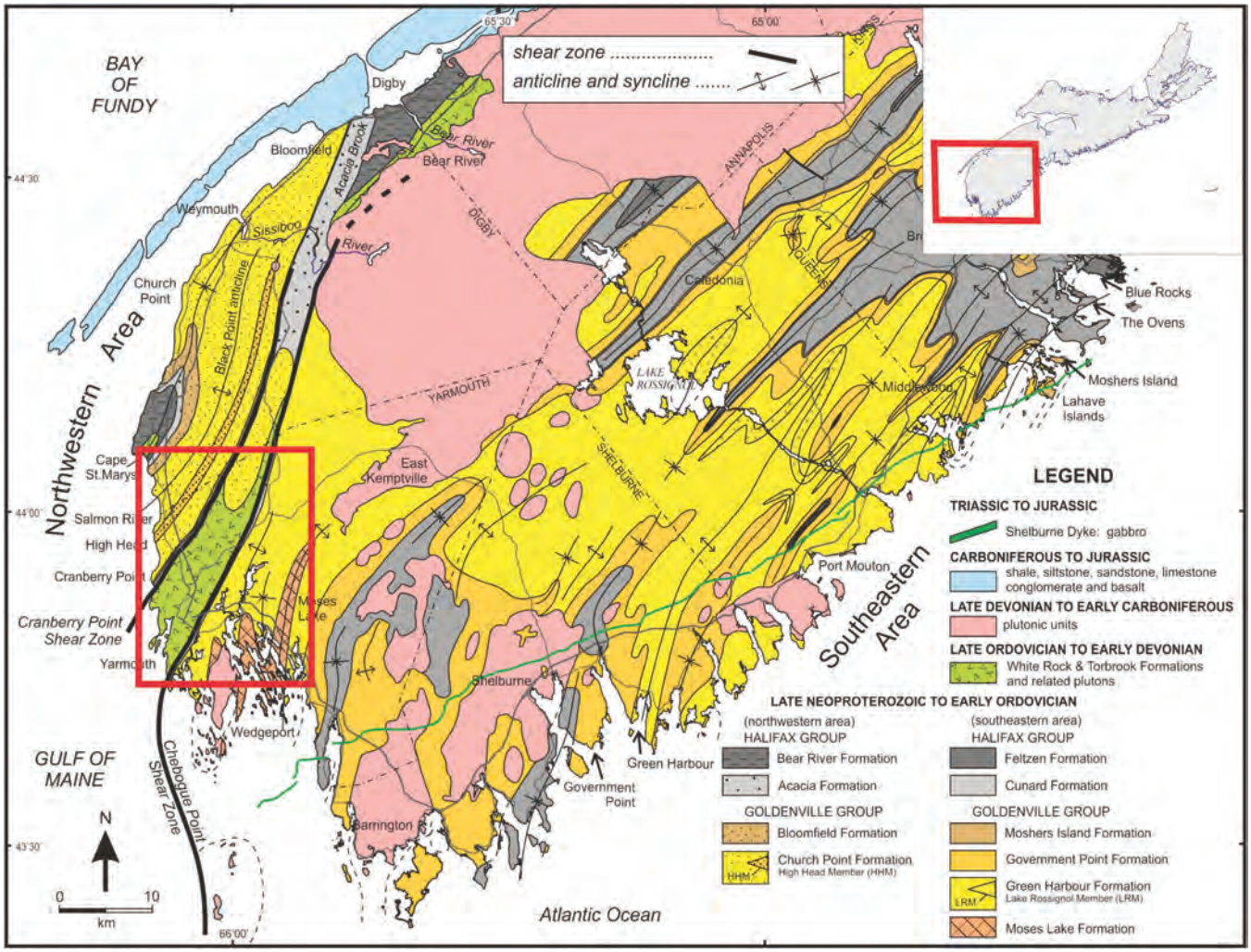

Figure 1. Bedrock geology of southwestern Nova Scotia (*modified from* White, 2010; White et al., 2018). The location of the study area is indicated by the red box.

exploration, not only in southwest Nova Scotia, but in recent (last 2 million years) glaciated terrain worldwide. In support of this research, regional-scale surficial geological mapping, sediment thickness modelling, till fabric and clast lithology analyses, till geochemistry, indicator minerals, and studies of glacial stratigraphy are being conducted to provide the regional context for interpreting results from the Brazil Lake case study. This report also includes data from previous till sampling studies in the Brazil Lake region by the NSDNRR in 2020 (Brushett and Tupper, 2021) and 2021 (Brushett et al., 2022).

Other Li occurrences/deposits globally may also contain other Li-silicates including lepidolite, petalite, and eucryptite (e.g. Steiner, 2019). Lithium in the Brazil Lake pegmatite is hosted in the clinopyroxene mineral, spodumene ($LiAlSi_2O_6$). Spodumene is the most sought after Li-bearing mineral for hard rock Li mining globally as it requires less energy to process than the Li-dominant trioctahedral mica, lepidolite [$K(Li,Al)_3Si_4O_{10}(OH,F)_2$] (Gao et al., 2023). The phyllosilicate mineral petalite ($LiAlSi_4O_{10}$) and the nesosilicate mineral eucryptite ($LiAlSiO_4$) are products of spodumene alteration (London and Burt, 1982; Charoy et al., 2001).

LOCATION AND ACCESS

The study area is located approximately 25 km northeast of Yarmouth, within the southwestern portion of the Atlantic Uplands of Nova Scotia, which is part of the Appalachian Region (Williams et al., 1974) in eastern Canada (Fig. 1). The topography consists of gently rolling hills with a nearly continuous cover of glacial sediments that is characterized by drumlin fields. The internal structure of several of these drumlins is exposed in coastal sections along the Yarmouth-Digby coast. Bedrock was only observed in a few places where it is exposed along stream beds and around the edges of bedrock quarries. Sample sites were accessed by truck along numerous local and resource-access roads, and recreational trails.

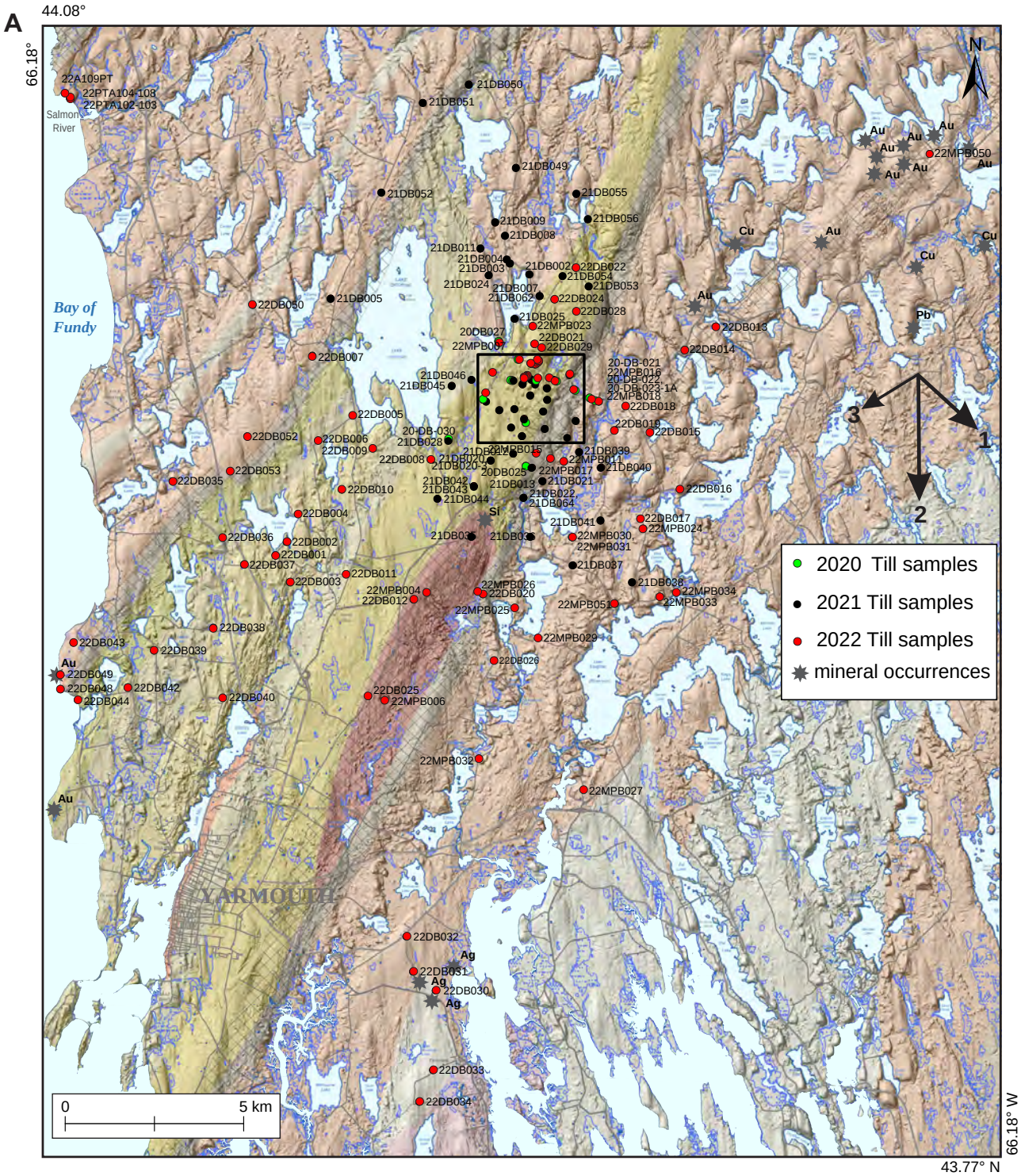

Legend

SILURIAN
- Brenton Pluton

ROCKVILLE NOTCH GROUP
WHITE ROCK FORMATION
- Government Brook Member
- Sunday Point Member
- Cape Fourchu Member
- Overton Member
- Chegoggin Point Member

UPPER CAMBRIAN TO LOWER ORDOVICIAN
HALIFAX GROUP
- Acacia Brook Formation

LOWER TO MIDDLE CAMBRIAN
GOLDENVILLE GROUP
- Bloomfield Formation
- Church Point Formation
- High Head Member
- Green Harbour Formation
- Shear Zones

Figure 2. a) Bedrock geology of the Brazil Lake study area (White et al., 2012) superimposed on a LiDAR hillshade image (azimuth of 315°) showing the location of till samples collected in 2020 (green dots), 2021 (black dots), and 2022 (red dots) and mineral occurrences (grey stars). Generalized ice-flow phases are shown by arrows and their relative age is indicated by numbers, with one being the oldest, based on regional ice-flow history by Stea and Grant (1982) and Finck and Stea (1995). Figure 2 continued on opposite page.

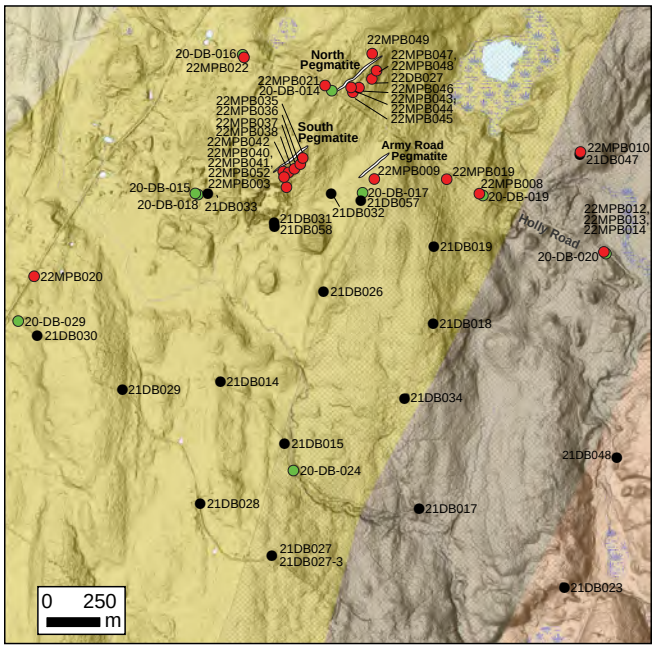

Figure 2 continued. b) The location of till samples inside the black box outlined in Figure 2a. The Brazil Lake and Army Road pegmatites are outlined by white polygons based on their known extents (Critical Raw Materials, 2023).

GEOLOGY

Bedrock geological setting

The study area is underlain by rocks of the Meguma terrane, the most easterly component of the northern Appalachian orogen (Hibbard et al., 2006; Fig. 2). The Meguma terrane is characterized by a thick sequence of Cambrian to Early Ordovician metasedimentary rocks, comprising the metasandstone-dominated Goldenville Group and the overlying siltstone- and slate-dominated Halifax Group (White, 2010). Locally, the Meguma Group is unconformably overlain by a thin sequence of Silurian to Early Devonian slate, quartzite, and volcanic rocks of the Rockville Notch Group (White and Barr, 2017; White et al., 2018). The earliest deformation occurred during the Middle Devonian Neoacadian orogeny (ca. 405–365 Ma) resulting in NE- to NNE-trending, upright regional-scale folds. The majority of these rocks were intruded by the ca. 373 Ma peraluminous South Mountain Batholith and related granitoid rocks (Fig. 1; White and Barr, 2017).

Local bedrock geology and mineralization

The Brazil Lake deposit is hosted by the Silurian White Rock Formation (Rockville Notch Group), comprising shallow marine metasedimentary rocks interbedded with minor mafic metavolcanic units, which locally include quartzite, amphibolite, and pelitic schist (Fig. 1, 2; White, 2010; White and Barr, 2017). The Breton Pluton, a syenogranite to monzogranite intrusion related to the White Rock Formation, is in fault contact with both the White Rock Formation and Halifax Group and occurs ~3 km southwest of the Brazil Lake deposit (Kontak, 2006). It is inferred to be Silurian based on U/Pb zircon age of 439 ±4 Ma (Keppie and Krogh, 2000). Numerous shear zones crosscut the area with the metamorphic grade increasing abruptly towards these shear zones. At the southeast margin of the White Rock Formation, staurolite-grade, typically schistose rocks are in faulted contact with slate of the Halifax Group that has been metamorphosed to amphibolite facies. The fault is inferred to be a brittle structure within the broader Chebogue Point Shear zone (previously termed the Deerfield shear zone). At its northwest margin, the Halifax Group and White Rock Formation are deformed along the Cranberry Point shear zone; cooling ages of muscovite indicate the deformation to be middle Carboniferous (Alleghanian) (Culshaw and Reynolds, 1997; Culshaw and Liesa, 1997; White and Barr, 2017). Field observations by Kontak (2006) suggest the Brazil Lake pegmatites were emplaced in an active shear zone where high-temperature ductile deformation occurred during consolidation of the pegmatite. Age dates of tantalite (U-Pb) from the South pegmatite indicate that pegmatite crystallization occurred at ca. 395 Ma (Kontak et al., 2005; Kontak and Keyser, 2009).

The bedrock geology of the Brazil Lake deposit is briefly described below and is summarized from studies of two separate northeast-trending, steeply dipping (to the southeast) pegmatite dykes that comprise the deposit. The dykes are named and described with respect to their location north or south of Holly Road (Kontak, 2004, 2006; Kontak et al., 2005). Drilling and surface trenching indicate that the North and South dykes, which are separated by about 300 m, occur as lenticular forms with wider cores transitioning to thinly tapered ends. The North dyke is at least 700 m in length and reaches a maximum thickness of 21 m at its centre. The South dyke has a defined strike length of ~300 m and a thickness of ~ 8–12 m. Both dykes have southwest-plunging trends of ~ 30–40° (Cullen et al., 2022).

The pegmatites are of albite-spodumene type and are characterized by coarse crystals of spodumene and K-feldspar, with intergranular spodumene (Fig. 3a), muscovite, albite, and quartz (Fig. 3b). Accessory phases include tantalite (Fig. 3c), tourmaline (Fig. 3d), apatite, beryl, sphalerite, and cassiterite. Spodumene ($LiAlSi_2O_6$), the most abundant lithium-bearing mineral in the pegmatites, is a light-coloured, relatively robust silicate mineral (H = 6.5–7) with two perfect cleavages, a vitreous luster that is pearly on its cleavage surface, and a moderate density of 3.18 g/cm^3. Key minerals in the pegmatites that could be useful indicator minerals for drift prospecting include black tourmaline, black tantalite, red garnet, blue apatite, green

Figure 3. a) Coarse-grained (≤0.5 m in length) white spodumene crystals exposed on the weathered subcropping surface of the South pegmatite (photograph by M.B. McClenaghan; NRCan photo 2022-571); **b)** fresh unweathered spodumene boulder extracted from the South pegmatite (photograph from Cullen et al. 2022); **c)** tantalite (black) crystals in quartz at the North pegmatite (photograph by D. Archibald, St. Francis Xavier University); **d)** cross-section of the South pegmatite in contact with the metavolcanic country rocks. At the outer contact of the pegmatite, abundant tourmaline is observed, which formed as a result of the exsolution of boron- rich fluids from the pegmatite.

beryl, cassiterite, wolframite, sphalerite, zircon, epidote, topaz, titanite, and phosphate minerals. Similarly, key trace elements that are typically enriched in LCT-type pegmatites and may be useful indicator elements include Li, Be, B, Mn, Rb, Y, Zr, Nb, Sn, Cs, La, Ce, Ta, Th, and U (Černý and Ercit, 2005).

Deposit discovery

The Brazil Lake pegmatites have been the focus of exploration and petrological studies since they were discovered in 1960 by tracing the source of pegmatite float boulders near what was later to be referred to as the South pegmatite (Taylor, 1967; Kontak, 2004; Barr and Cullen, 2010). Numerous spodumene-bearing boulders are still evident on-surface down-ice of the North pegmatite (Fig. 4). The most recent resource estimate for the two pegmatites was reported as measured and indicated resources of 555 300 tonnes grading 1.30% Li_2O and an inferred mineral resource of 381 000 tonnes grading 1.48% Li_2O (Cullen et al., 2022; Canadian Mining Journal, 2022). Diamond drilling was initiated in October of 2022 to further define the Li resources at the South and North pegmatites and to access the Li potential of a third nearby pegmatite, the Army Road pegmatite (Fig. 2b). At the time of writing of this report, drilling continued to expand the South

Figure 4. Abundant spodumene-bearing float boulders are exposed on the surface south and east of the North Pegmatite. Photograph by Beth McClenaghan, NRCan photo 2022-589.

pegmatite down-plunge to the southwest with thicknesses up to 20 m and, identified spodumene in the Army Road pegmatite, 500 m to the east, that remains open down-plunge to the southwest (Critical Raw Materials, 2023).

Surficial geology

Extensive till cover throughout much of southwestern Nova Scotia has made bedrock mapping and exploration for buried mineralization challenging. The areal extent of the pegmatites at the Brazil Lake pegmatite deposit is not well known due to till cover, which limits their outcrop exposure. The study area underwent extensive glacial modifications through the late Wisconsin glaciation leaving thick glacial sediments and complex landforms. South-southeast-trending drumlins are the predominant glacial landform over much of the region, with the orientation transitioning to south trending drumlins close to the coastline.

Till thickness is variable, ranging from thin veneers (<2 m) over the pegmatites to drumlin ridges composed of over 40 m of till (Brushett et al. in prep). In the Brazil Lake area, mega-scale glacial lineations were also identified in the LiDAR imagery of this drumlin-

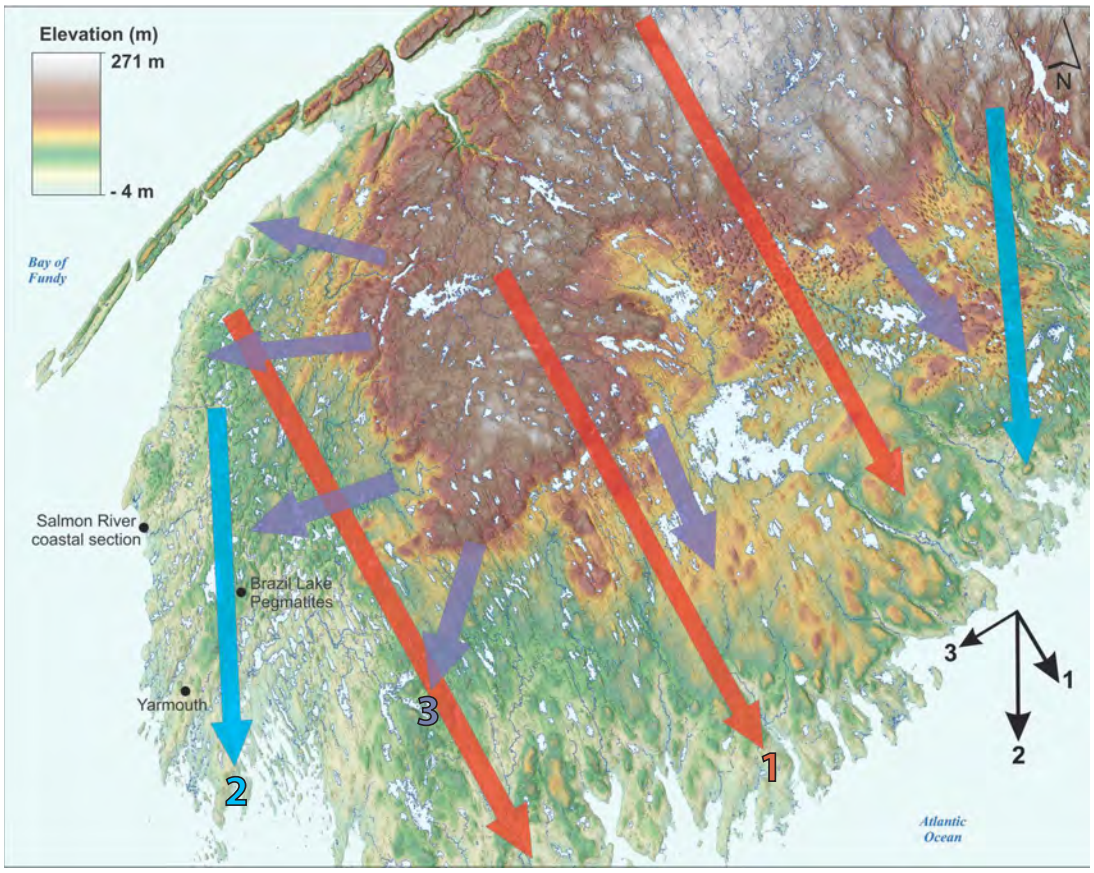

Figure 5. Generalized ice-flow chronology of southern Nova Scotia (Stea and Grant, 1982; Finck and Stea, 1995; Stea et al., 2011).

ized terrain, indicative of fast flowing ice during the latter phases of glaciation (i.e. ice streaming: Stokes and Clark, 2002; Fig. 5). The area between these till lineations (till ridges) is characterized by thin till overlying bedrock with sediment cover of <5 m. Glaciofluvial deposits commonly occur in topographic lows, which are now occupied by modern rivers and wetlands.

The current knowledge of the glacial history of southwestern Nova Scotia is largely derived from previous regional-scale (1:100 000) surficial mapping and till sampling conducted by Stea and Grant (1982) and Finck and Stea (1995) in the 1970s and 1980s. This mapping and sampling, together with the stratigraphic studies by Grant (1976), Grant and King (1984), and Stea et al. (1992), have led to a broad framework of the regional glacial history. This stratigraphic framework was based upon the traditional layer-cake model of till stratigraphy and should be re-examined in the context of the time-transgressive nature and evolution of the former ice sheet during its early growth, full extension, and decay. Drift thickness modelling (Brushett et al. in prep) and new regional surficial mapping, aided by LiDAR data, are ongoing by NSDNRR to update the stratigraphic model for the region.

The surficial geology of southwestern Nova Scotia is the product of multiple glacial advances and retreats throughout several glacial events (Stea, 2004; Stea et al., 2011). Multiple till units, identified in coastal sections in southwest Nova Scotia, reflect several phases of glacial deposition and shifting ice-flow directions (Grant, 1980; Stea and Grant, 1982), which are described below from oldest to youngest:

1) The oldest ice-flow phase (Northumberland phase; Marine Isotope Stage (MIS) 6: ca. 190–130 ka), identified from the lowermost grey silty till at the base of some coastal sections, was interpreted to have been deposited by east to southeast ice-flow sourced from the northern Appalachian Mountains (Stea et al., 2011).
2) Regional east to southeastward ice-flow from New Brunswick during the Caledonia phase (MIS 4; ca. 75–50? ka) was responsible for the early formation of drumlins in southwest Nova Scotia. These drumlins are silt- and clay-rich (as well as shell-rich in coastal sections) and contain a high percentage of foreign bedrock components with transport distances of >80 km (Stea and Finck, 2001; red arrows in Fig. 5).
3) Subsequent southward regional ice-flow during the Escuminac phase (MIS 2; 22–18 ka) modified older drumlins and formed new ones that reflect a more southward flow (blue arrows in Fig. 5).

Figure 6. Examples of subglacial traction (lodgement) till sampled at various sites in the Brazil Lake study area. Note the compaction of the till as demonstrated by fissility and overconsolidation. Width of shovel head is 21 cm: a) site 22MPB026 after sampling; b) site 22MPB036, overconsolidated chunks of till on the shovel. Note the white spodumene clast indicated by the yellow arrow; c) site 22MPB027 after sampling showing well developed A, B, and C soil horizons; d) 22MPB027 overconsolidated chunk of till on shovel; e) site 22MPB-038 after sampling showing subhorizontal fissility behind the shovel. Photographs by M.B. McClenaghan, NRCan photo 2023-061, 2023-062, 2023-063, 2023-064, and 2023-065, respectively).

reflect a more southward flow (blue arrows in Fig. 5).

4) During the following Scotian phase (ca. 20–17 ka), regional ice centres shifted, and Nova Scotia was cut off from external ice centres (i.e. the Laurentide Ice Sheet) mainly due to ice streaming in marine channels (Shaw et al., 2006; Stea et al., 2011). The resultant Scotian Ice Divide formed lengthwise down the centre of the province such that ice-flow direction varied from southwest to southeast in southwestern Nova Scotia (Grant, 1980; Stea and Grant, 1982; purple arrows in Fig. 5).

Figure 7. Spodumene clasts from the pegmatites were readily visible while sampling tills in backhoe trenches just down-ice of the pegmatites (photograph by M.B. McClenaghan, NRCan photo 2022-590).

Till characteristics

Four main genetic properties were used to differentiate till facies: 1) matrix texture, 2) fissility and compaction, 3) clast lithologies, and 4) the proximity to geomorphic forms that could be identified using LiDAR imagery. Using these criteria, two till facies were observed in this study.

One of the till facies is silty sand that is over consolidated and sometimes displays subhorizontal fissility with visible jointing (Fig. 6). A typical till exposure (~1–-2 m depth) shows a very compact light brownish grey silty-sandy till with angular to subrounded clasts, the majority of which reflect local bedrock lithologies, with numerous striated and faceted clasts. This till can be classified as a subglacial traction till, a term that supersedes ‘subglacial lodgement till’ in the modern literature (e.g. Evans, 2017; McClenaghan et al., 2023c). Pebbles and cobbles of spodumene were observed in this till facies (Fig. 6b, 7) in trenches just down-ice of the North and South pegmatites. A bedrock subcrop surface revealed by previous stripping of the South pegmatite is glacially polished and striated (179°) and demonstrates that the bedrock here was in

Figure 8. A striated bedrock surface that was exposed during previous stripping of the South pegmatite (photograph by D. Brushett, Nova Scotia Dept. Natural Resources and Renewables). The marker is 13.7 cm for scale.

direct contact with southward-flowing ice (Fig. 8). This facies is the primary target sample medium.

A second till facies was identified, primarily in quarries and drumlin exposures where it is seen as a thin (<2 m) horizon on the drumlin flanks (area within the yellow dashed lines in Fig. 9). This till is sandier, less indurated, less compact, and contains well sorted lenses and layers of sand (Fig. 9, 10). A higher proportion of clasts and larger range of clast sizes, which are also more monolithic than the subglacial traction facies, were also identified. In some quarries, a boulder horizon was identified near and at the surface, generally composed of angular greywacke boulders (Fig. 9b) This till can be classified as a subglacial melt-out till (e.g. Evans, 2017; McClenaghan et al., 2023c). Note that no supraglacial tills (i.e. debris sheared and carried up into the glacier as englacial load or debris deposited on top of the glacier during transport) were observed anywhere in region.

A ternary diagram showing the percentage of sand, silt, and clay in the till matrix of the samples highlights a continuum from a sandy silt to a silty sand (Fig. 11). Finer grained tills with a higher clay content occur in the western part of the study area. This is likely due to these tills being derived from ice flowing across the Gulf of Maine and Bay of Fundy entraining fine-grained Carboniferous red bed sediments, which is reflected in the reddish hue in the tills observed in coastal sections as well as marine shells and shell fragments.

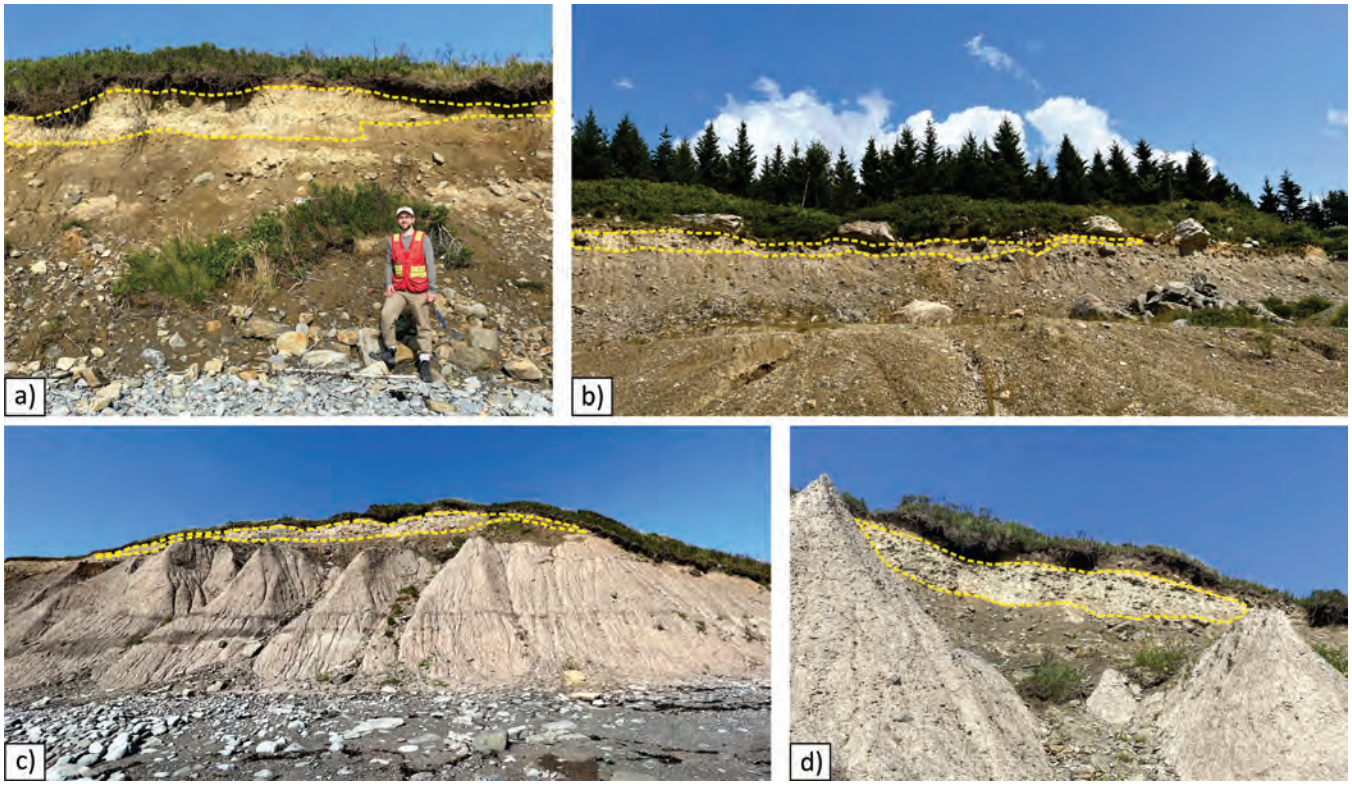

Figure 9. a) Subglacial melt-out till (outlined by a yellow dashed line) that was observed as a thin (<2 m) horizon containing well sorted lenses and layers of sand in a coastal section (Beaver River till type locality). **b)** Upper melt-out till observed in a quarry section showing loose, sorted sandy lenses and beds. Clasts and boulders from this horizon are generally composed of locally derived angular greywacke boulders. **c)** A thin upper melt-out till horizon, which was only identified on the southeastern flank of a drumlin from the Salmon River coastal section (*see* Fig. 2, 22PTA series samples). **d)** Close-up view of the upper melt-out till facies from Salmon River costal section showing pale sandy till with abundant local, mostly angular clast lithologies. Photographs by D. Brushett, Nova Scotia Department of Natural Resources and Renewables.

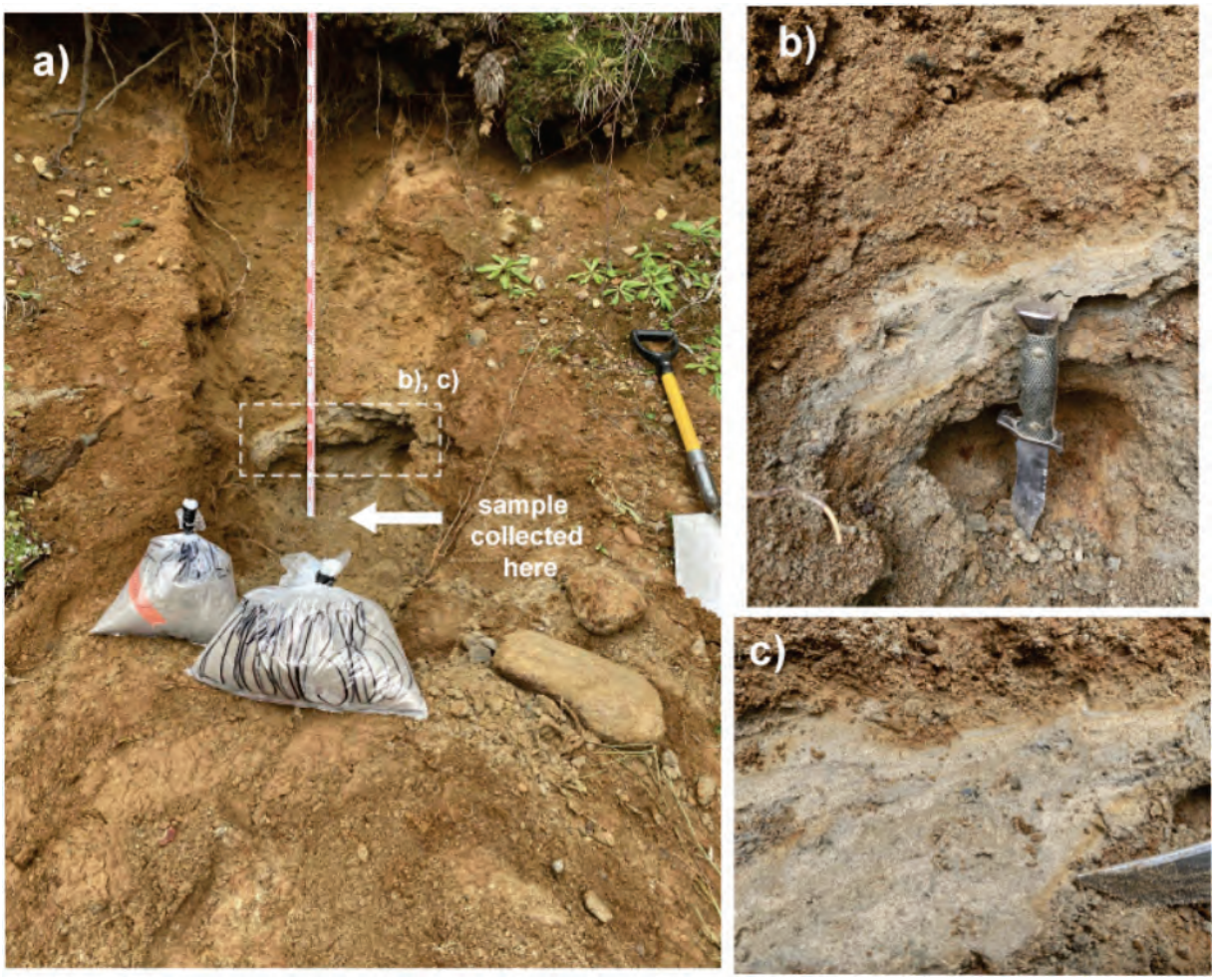

Figure 10. a) Photograph of the of subglacial melt-out till sampled at site 22MPB023. Subglacial melt-out till is typically looser than subglacial traction till and also contains lenses of sorted sand (**b** and **c**) within the till. The red and white sections on the measuring tape are 10 cm long. Photographs by Jessey Rice: a) NRCan photo 2023-066, b) NRCan photo 2023-067, and c) NRCan photo 2023-068).

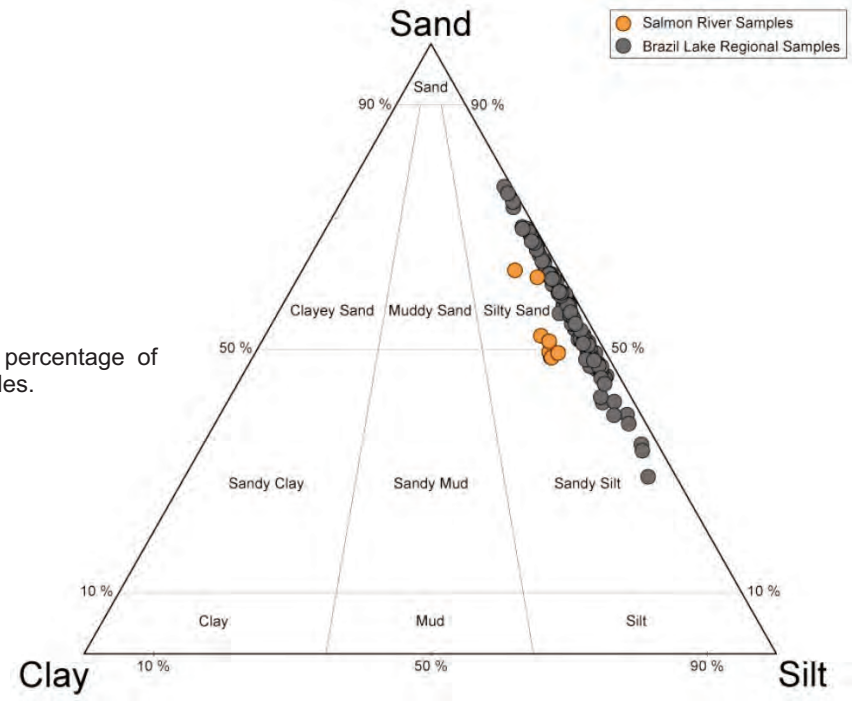

Figure 11. Ternary diagram showing the percentage of sand, silt, and clay in the matrix of till samples.

PREVIOUS SURFICIAL GEOCHEMICAL AND MINERALOGICAL STUDIES

The first till geochemical study in the Brazil Lake area was conducted by Shell Resources in 1981 when till sampling (B-horizon) was conducted over the pegmatites at 50 m intervals on 100 m spaced east-west lines. The 0.177–2.0 mm fraction was pulverized to <0.074 mm and analyzed for Sn and Ta by XRF and Li by multi-acid digestion/atomic absorption spectrometry (AAS). The highest content of Li, Sn, and Ta reported was 228, 152, and 46 ppm, respectively (Palma et al., 1982). A regional lake sediment study of the Meguma terrane, including the area around Brazil Lake, did not show any pronounced geochemical anomaly for Li, F, Rb, Nb, Sn, or W (Rogers et al., 1985, 1990).

A multimedia geochemical study (till, balsam fir twigs, and humus) was conducted over a 600 x 600 m sampling grid (~100 m sample spacing for till, 50 m for twigs and humus) overlying the pegmatites by MacDonald et al. (1992). The <0.063 mm till fraction was analyzed by several methods, including instrumental neutron activation analysis (INAA), multi-acid digestions, a variety of fusions, and XRF for several pathfinder elements of rare-element pegmatites, including Li, B, Be, F, P, Fe, Rb, Nb, Cs, Ta, and Sn (*see* Table 4 *in* McDonald et al., 1992). The authors also analyzed the 0.063–0.25 mm >2.95 specific gravity (SG) heavy mineral fraction of the till using the same methods. They reported a variable geochemical response between the different sample media with "spotty" zones of enrichment of limited areal extent, which they attributed to the small size of the pegmatite veins and limited glacial dispersal. A contrast in Li and Cs concentrations was also noted, with higher concentrations of Li and Cs near the South pegmatite, whereas only Li was elevated near the North pegmatite, suggesting different mineralogical assemblages.

Till surveys of the pegmatite area conducted by Lundrigan (2008) included several till size factions, which were analyzed by aqua regia, multi-acid, Li-metaborate fusion and Na-peroxide fusion with ICP-MS analyses. Lundrigan (2008) reported that Li was the only pathfinder element identified with anomalously high concentrations in till overlying, and up to 400 m southeast, of the pegmatites. The highest concentrations (>777 ppm) and geochemical contrast was observed in the coarse-grained (-1.0+0.5 mm) till fraction.

Ongoing exploration by Champlain Mineral Ventures since 2002 has included several till and soil sampling programs (Black, 2011, 2012; Wightman, 2018, 2020). B-horizon soil sampling (<177 µm fraction) collected at 25 m spacing along 100 m spaced lines

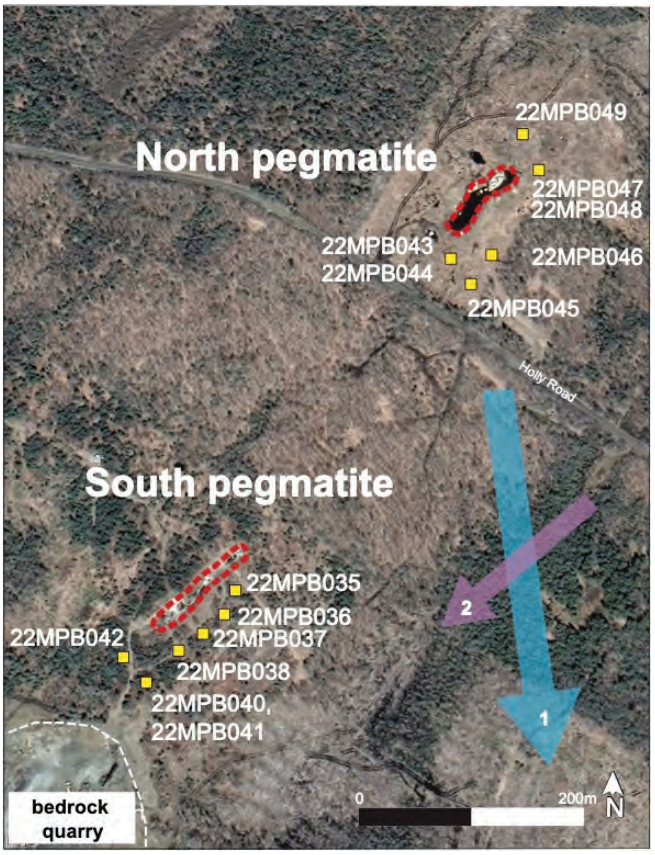

Figure 12. Location of GSC till samples collected in 2022 in backhoe trenches excavated proximal to the North and South pegmatites. Pegmatite subcrops exposed by previous stripping are outlined by dashed red lines. Regional ice-flow directions are indicated by arrows in the bottom right corner of the figure: (1) older flow, (2) younger flow. From McClenaghan et al. (2023b). See regional map in Figure 2a and detailed map in 2b for location.

(multi-acid and Na-peroxide fusion/ICP-MS), Soil Gas Hydrocarbon (SGH) soil sampling, and spodumene grain counts from bulk till samples were conducted to define new spodumene-bearing pegmatite targets. Spodumene grain counts recovered centimetre-sized spodumene grains, which were interpreted to indicate glacial dispersal from the north-northwest; however, grain counts were not normalized to sample weight.

METHODS

Till sampling

In 2020, 2021, and 2022, 184 till samples, including field duplicates, were collected from 171 sites (Fig. 2; Appendix B3 map) from hand-dug pits, and till exposures in borrow pits or along local roads. Some of the samples were also collected from backhoe trenches dug on the down-ice (SSE) side of both the North and South pegmatites where C-horizon (unoxidized to moderately oxidized) till was targeted (Fig. 12). Till samples were collected by NSDNRR (DB series sample numbers) and the GSC (MPB series sample num-

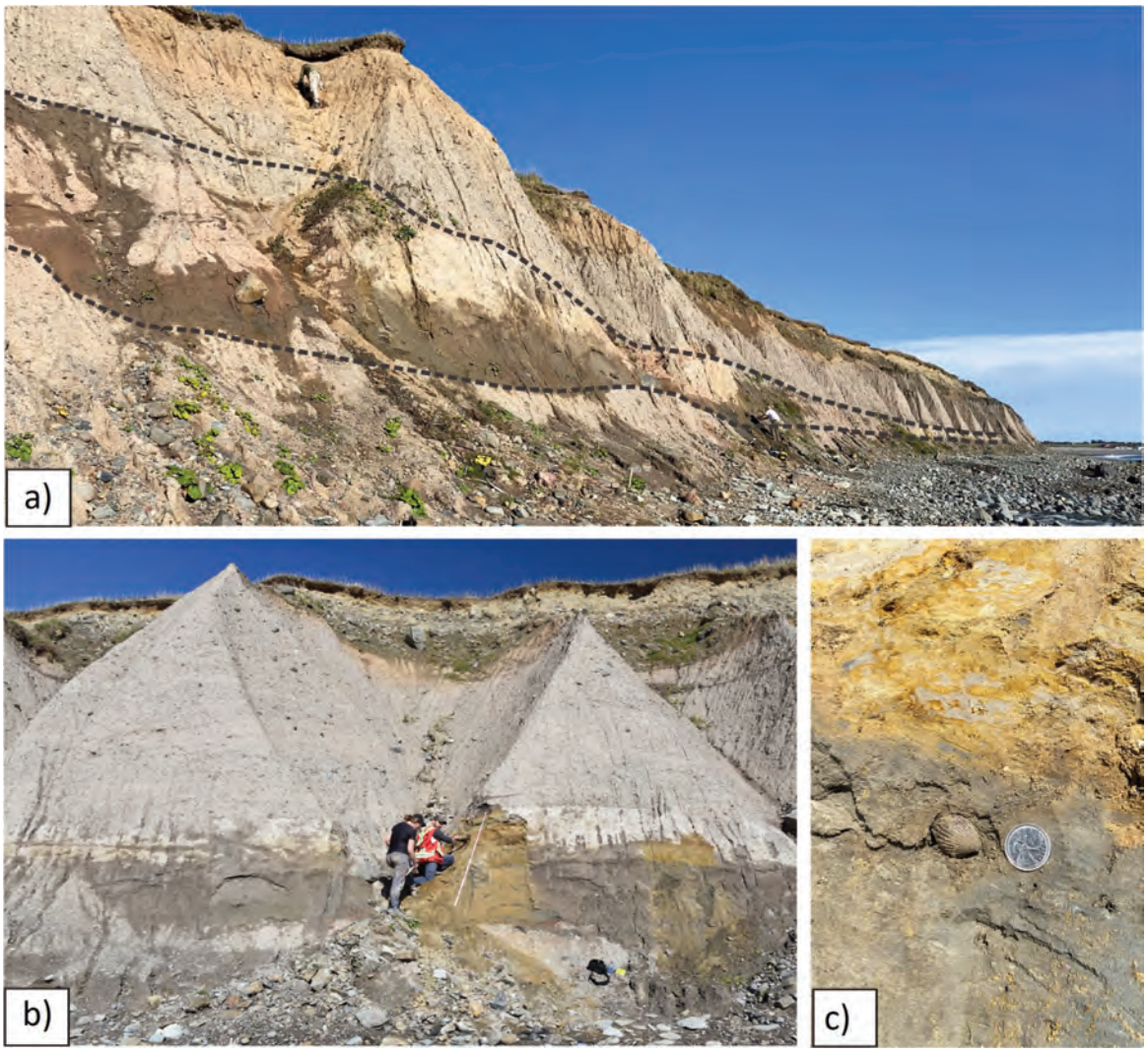

Figure 13. a) Salmon River sand unit showing the location of an optical stimulated luminescence (OSL) dating sample site. The photograph shows a Salmon River section looking south with the middle sand unit highlighted between the black dashed lines. Scale as indicated by person at the top of section. Photograph by D. Brushett, Nova Scotia Dept. Natural Resources and Renewables; **b)** Salmon River sand unit showing the location of an OSL dating sample site. The sand unit transitions upwards from a lower, grey, well sorted, fine-grained sand facies with abundant shells and shell fragments to a beige to orange-brown, medium-grained sandy facies with fewer shell fragments. Photograph by Roger Paulen, NRCan photo 2023-060; **c)** several larger intact shells were collected for dating and identification. Scale indicated by a 25 cent coin with a diameter of 23.88 mm. Photograph by D. Brushett, Nova Scotia Dept. Natural Resources and Renewables.

bers) following the Geological Survey of Canada till sampling protocols described in Spirito et al. (2011), Plouffe et al. (2013), and McClenaghan et al. (2020, 2023c). At each site, a small 3–6 kg sample was collected for characterization (Munsell colour and grain size data) and geochemical analysis of the till matrix, and for archiving. Field duplicates were collected at selected sites. At 87 of the sites, an additional 10–15 kg till sample was collected for the recovery of indicator minerals of Li-bearing pegmatite and separation of pebbles for lithological analysis (>2.0 mm fraction). The indicator mineral and pebble lithology results will be presented in a separate report.

General metadata for the till samples are reported in Appendix A. Field data were collected at each site and are reported in Appendix B1, which includes GPS coordinates, general site description, sample description [soil horizon, texture, colour, clast types, relative percentages of clasts, matrix description (i.e. percent sand, silt, clay), and sample depth]. Site photos for samples collected in 2021, 2022, and 2023 are included in Appendix B2. No site photos are available for samples collected in 2020. A detailed sample location map is included in Appendix B3.

At one coastal section of the mouth of the Salmon River (Fig. 13), ~25 km north of Yarmouth and ~16 km west of the Brazil Lake pegmatites, approximately 19 m of glacial and non-glacial sediments are exposed overlying bedrock. Seven 3 kg till samples (PTA sample number series) and accompanying bags of pebbles

(1–4 cm in size) were collected from this section to document the geochemical and textural characteristics of the multiple till units (Appendix B3 map). No heavy mineral samples were collected. Data from these till samples and pebbles will be compared to regional till samples and samples from the Brazil Lake area to further our understanding of the regional glacial history and ice-flow patterns. Two till fabrics studies were conducted in the lowermost till and will be discussed in a later report. An additional three sand samples were collected for Optically Stimulated Luminescence (OSL) dating from a large continuous shelly sand bed that occurs between the lowermost till layer and the tills that were deposited above it (Fig. 13b, c). These sand beds, known as the Salmon River sand, have had very limited previous research (Grant, 1976), and have been the subject of mixed interpretations as to their age, ranging from the last interglacial (Stea et al., 1992) to a younger interstadial deposit (Grant, 1987).

Sample processing

Till samples for geochemical and till matrix characterization were shipped to the GSC Sedimentology Lab in Ottawa where they were air dried after being laid out on dry Kraft paper and, if needed, disaggregated inside a plastic sample bag using a rubber mallet (Girard et al., 2004). After drying, an ~800 g split was archived and the remainder of each sample was subjected to matrix grain-size analysis, Munsell colour determination, and dry sieving in preparation for geochemical analysis. Matrix grain-size analysis (% sand, silt, and clay) was conducted using a Lecotrac LT-100 Particle Size Analyzer (reported in Appendix B1). The Munsell colour of each sample (moist) was determined using a spectrophotometer linked to IQC colour software (*see* Appendix B1). Dry sieving was completed using stainless steel US standard sieves to recover the <0.002, <0.063, and 1.0–2.0 mm fractions in 2020 and the <0.063 and 1.0–2.0 mm fractions in 2021 and 2022. GSC protocols for sieve cleaning during sample preparation are outlined in Grenier et al. (2015).

Geochemical analysis

The analytical methods used in this study are summarized in Table 1. Methods, lower and upper detection limits, and units of measure are listed in Table 2. Method descriptions are listed in Appendix C.

In 2020, the <0.002, <0.063, and 1.0–2.0 mm fractions of till samples were analyzed for a suite of major, minor, and trace elements at Bureau Veritas Minerals Canada, Vancouver. The 1.0–2.0 mm fraction was pulverized to approximately 0.74 mm before analysis. Analytical methods included the following:

1) modified aqua regia digestion ($HCl:HNO_3:H_2O$ in a 1:1:1 ratio) followed by an ICP-MS analysis (BV AQ252 package on 30 g);
2) 4-acid digestion, followed by ICP-MS determination (BV MA250 package); and
3) Li-metaborate fusion followed by nitric acid digestion followed by ICP-MS analysis (BV LF200 package).

In the subsequent years of 2021 and 2022, the <0.063 mm and 1.0–2.0 mm fractions of each till sample were analyzed for a suite of major, minor, and trace elements at Bureau Veritas Minerals Canada (Vancouver) and SGS Canada Inc. (Burnaby). The 1.0–2.0 mm fraction was pulverized to approximately 0.74 mm before analysis. Analytical methods included the following:

1) a modified aqua regia digestion ($HCl:HNO_3:H_2O$ in a 1:1:1 ratio) followed by ICP-ES and ICP-MS analyses (BV AQ252/250+REE package on 30 g or 0.5 g);
2) 4-acid digestion, followed by an ICP-ES and ICP-MS analysis (BV MA250 package); and
3) Na-peroxide fusion followed by ICP-OES and ICP-MS analyses (SGS GE_ICM90A50 and GE_IMS90A50 package) at SGS Canada.

Blind (analytical) laboratory duplicates were inserted into the batches by the GSC Sedimentology Laboratory to monitor analytical precision. A summary of the GSC laboratory duplicate data is presented in Appendix H (sheets AR_Dups, NaF_Dups, and 4A_Dups).

This study employed a variety of certified till reference standards, including TILL-1, TILL-4, and OREAS 750. TILL-1 and TILL-4 are CANMET certified standards. Additionally, a Li-pegmatite standard, OREAS-750, was used to monitor results for Li and other critical metals associated with LCT pegmatites. However, analyses indicated that OREAS-750 is only ideal for Na-peroxide fusion, as the concentration of Li in this standard is above the upper limit of detection for aqua regia and 4-acid digestions. GSC-inserted laboratory reference standard data are presented in Appendix H in worksheets labelled as Till-4, Till-1, and OREAS-750. Silica sand blanks were inserted into all analytical batches by the GSC Sedimentology Lab prior to sieving and analyses, generally at the start, middle, and end of batches, to monitor potential cross contamination between samples during sieving and/or during analyses. The data for blanks are reported in Appendix H.

Portable XRF (pXRF) lab-based analysis on sieved fractions of 63 till samples (including blanks and reference materials) and 1.0–2.0 mm pulverized fractions from the MPB 2022 series samples were conducted by the GSC Inorganic Research Laboratory. Analysis was done using an Innov-X DP4000 handheld XRF Analyzer (serial 510964) equipped with a Moxtek Ta X-Ray tube and a Ketek 30 mm^2 detector. Samples were run in "3 Beam Soil" Mode, with 60 s real time

Table 1. Summary of analytical methods, size fractions, analytical lab report numbers and the location of data reported in appendices.

Digestion/ method	Sample year	Lab	Sample sequence	Organization	Size fraction	Lab's analytical code	Aliquot mass	Report received	Lab report number	Source of data	Appendix file
Aqua regia	2020	Bureau Veritas	20DB014 to 20DB030	NSDNRR	<0.002 mm	AQ252-EXT,+REE	30 g	30-Apr-21	VAN21000508	Brushett et al. 2022	Appendix D1
	2020	Bureau Veritas	20DB014 to 20DB030	NSDNRR	<0.063 mm	AQ252-EXT,+REE	30 g	8-Apr-21	VAN21000506	Brushett et al. 2022	Appendix D1
	2020	Bureau Veritas	20DB014 to 20DB030	NSDNRR	1-2 mm	AQ252-EXT,+REE	30 g	1-Apr-21	VAN21000507	Brushett et al. 2022	Appendix D1
	2021	Bureau Veritas	21DB002 to 21DB058	NSDNRR	<0.063 mm	AQ250-EXT, +REE	0.5 g	3-Feb-23	VAN23000186	this report	Appendix D1
	2021	Bureau Veritas	21DB002 to 21DB058	NSDNRR	1-2 mm	AQ250-EXT, +REE	0.5 g	3-Feb-23	VAN23000186	this report	Appendix D1
	2022	Bureau Veritas	22DB001 to 22DB056	NSDNRR	<0.063 mm	AQ252-EXT,+REE	30 g	6-Feb-23	VAN23000187	this report	Appendix D1
	2022	Bureau Veritas	22MPB001 to 22MPB053 22PTA101 to 22PTA109	GSC	<0.063 mm	AQ250-EXT, +REE	0.5 g	3-Feb-23	VAN23000186	this report	Appendix D1
	2022	Bureau Veritas	22MPB001 to 22MPB053	GSC	1-2 mm	AQ250-EXT +REE	0.5 g	13-Feb-23	VAN23000250	this report	Appendix D1
4-acid	2020	Bureau Veritas	20DB014 to 20DB030	NSDNRR	<0.002 mm	MA250	0.25 g	30-Apr-21	VAN21000508	Brushett et al. 2022	Appendix D2
	2020	Bureau Veritas	20DB014 to 20DB030	NSDNRR	<0.063 mm	MA250	0.25 g	8-Apr-21	VAN21000506	Brushett et al. 2022	Appendix D2
	2020	Bureau Veritas	20DB014 to 20DB030	NSDNRR	1-2 mm	MA250	0.25 g	1-Apr-21	VAN21000507	Brushett et al. 2022	Appendix D2
	2022	Bureau Veritas	22DB001 to 22DB056	NSDNRR	<0.063 mm	MA250	0.25 g	6-Feb-23	VAN23000187	this report	Appendix D2
	2022	Bureau Veritas	22MPB001 to 22MPB053	GSC	<0.063 mm	MA250	0.25 g	9-May-23	VAN23000852	this report	Appendix D2
reanalysis	2023	Bureau Veritas	22MPB001 to 22MPB013	GSC	<0.063 mm	MA250	0.25 g	13-Jun-23	VAN23001111	this report	merged into Appendix D2
	2022	Bureau Veritas	22MPB001 to 22MPB053	GSC	1-2 mm	MA250	0.25 g	9-May-23	VAN23000852	this report	Appendix D2
Na-peroxide fusion	2021	SGS	21DB002 to 21DB058	NSDNRR	<0.063 mm	GE_ICP90A50, GE_IMS90A50		10-Mar-22	BBM22-15771	this report	Appendix D3
	2021	SGS	21DB002 to 21DB058	NSDNRR	1-2 mm	GE_ICP90A50, GE_IMS90A50		10-Mar-22	BBM22-15938	this report	Appendix D3
	2022	SGS	22DB001 to 21DB056	NSDNRR	<0.063 mm	GE_ICP90A50, GE_IMS90A50		16-Mar-23	BBM23-25458	this report	Appendix D3
	2022	SGS	22MPB001 to 22MPB053	GSC	<0.063 mm	GE_ICP90A50, GE_IMS90A50		16-Mar-23	BBM23-25458	this report	Appendix D3
	2022	SGS	22MPB001 to 22MPB053	GSC	1-2 mm	GE_ICP90A50, GE_IMS90A50		13-Mar-23	BBM23-25716	this report	Appendix D3
Li meta/tetraborate fusion	2020	Bureau Veritas	20DB014 to 20DB030	NSDNRR	<0.002 mm	LF200		30-Apr-21	VAN21000508	Brushett et al. 2022	Appendix D4
	2020	Bureau Veritas	20DB014 to 20DB030	NSDNRR	<0.063 mm	LF200		8-Apr-21	VAN21000506	Brushett et al. 2022	Appendix D4
	2020	Bureau Veritas	20DB014 to 20DB030	NSDNRR	1-2 mm	LF200		1-Apr-21	VAN21000507	Brushett et al. 2022	Appendix D4
pXRF	2022	GSC	22MPB001 to 22MPB053 22PTA-101 to 22PTA-109	GSC	<0.063 mm	pXRF soil mode		13-Feb-23	20225	this report	Appendix E1
	2022	GSC	22MPB001 to 22MPB053 22PTA-101 to 22PTA-109	GSC	1-2 mm	pXRF soil mode		13-Feb-23	20225	this report	Appendix E1

NSDNRR = Nova Scotia Department of Natural Resources and Renewables
GSC = Geological Survey of Canada

Table 2. The lower and upper detection limits for the <0.002, <0.063 (silt + clay), and 1.0–2.0 mm (coarse) sized fractions of till for samples collected in 2020, 2021, and 2022.

		Lower detection limit				Upper detection limit			
Element	Unit	Aqua regia	4-acid	Na peroxide	Li borate	Aqua regia	4-acid	Na peroxide	Li borate
Ag	ppm	0.002	0.02	5	ND	100	200	200	ND
Al	wt. %	0.01	0.01	0.01	0.01	10	20	25	100
As	ppm	0.1	0.2	3	ND	10000	10000	10000	ND
Au	ppb	0.2	ND	ND	ND	100000	ND	ND	ND
B	ppm	20	ND	ND	ND	2000	ND	ND	ND
Ba	ppm	0.5	1	10	1	10000	10000	50000	50000
Be	ppm	0.1	1	5	1	1000	1000	25000	10000
Bi	ppm	0.02	0.04	0.1	ND	ND	4000	1000	ND
Ca	wt. %	0.01	0.01	0.1	0.01	40	40	25	100
Cd	ppm	0.01	0.02	0.2	ND	2000	4000	10000	ND
Ce	ppm	0.1	0.02	0.1	0.1	2000	2000	10000	50000
Co	ppm	0.1	0.2	0.5	0.2	2000	4000	10000	10000
Cr	ppm	0.5	1	20	0.002	10000	10000	50000	10
Cs	ppm	0.02	0.1	0.1	ND	2000	2000	10000	ND
Cu	ppm	0.01	0.1	10	ND	10000	10000	50000	ND
Dy	ppm	0.02	0.1	0.05	0.05	2000	2000	1000	10000
Er	ppm	0.02	0.1	0.05	0.03	2000	2000	1000	10000
Eu	ppm	0.02	0.1	0.05	0.02	2000	2000	1000	10000
Fe	wt. %	0.01	0.01	0.01	0.04	40	60	25	100
Ga	ppm	0.1	0.02	1	0.5	1000	100	1000	10000
Gd	ppm	0.02	0.1	0.05	0.05	1000	2000	1000	10000
Ge	ppm	0.1	ND	1	ND	100	ND	1000	ND
Hf	ppm	0.02	0.02	ND	0.1	1000	1000	ND	10000
Hg	ppb	5	ND	ND	ND	50000	ND	ND	ND
Ho	ppm	0.02	0.1	0.05	0.02	2000	2000	1000	10000
In	ppm	0.02	0.01	0.2	ND	1000	1000	1000	ND
K	wt. %	0.01	0.01	0.1	0.01	10	10	25	100
La	ppm	0.5	0.1	0.1	0.1	10000	2000	10000	50000
Li	ppm	0.1	0.1	10	ND	2000	2000	50000	ND
Lu	ppm	0.02	0.1	0.05	0.01	2000	2000	1000	10000
Mg	wt. %	0.01	0.01	0.01	0.01	30	30	25	100
Mn	ppm	1	1	10	0.01	10000	10000	100000	30
Mo	ppm	0.01	0.05	2	ND	2000	4000	10000	ND
Na	wt. %	0.001	0.001	ND	0.01	5	10	ND	100
Nb	ppm	0.02	0.04	2	0.1	2000	2000	10000	1000
Nd	ppm	0.02	0.1	0.1	0.3	2000	2000	10000	10000
Ni	ppm	0.1	0.1	10	20	10000	10000	100000	10000
P	wt. %	0.001	0.001	0.01	0.01	5	5	25	100
Pb	ppm	0.01	0.02	2	ND	10000	10000	50000	ND
Pd	ppb	10	ND	ND	ND	100000	ND	ND	ND
Pr	ppm	0.02	0.1	0.05	0.02	2000	2000	10000	10000
Pt	ppb	2	ND	ND	ND	100000	ND	ND	ND
Rb	ppm	0.1	0.1	2	0.1	2000	2000	10000	10000
Re	ppb	1	2	ND	ND	10000	100000	ND	ND
S	wt. %	0.02	0.04	ND	ND	10	10	ND	ND
Sb	ppm	0.02	0.02	1	ND	2000	4000	10000	ND
Sc	ppm	0.1	0.1	5	1	100	200	50000	10000
Se	ppm	0.1	0.3	ND	ND	100	1000	ND	ND
Si	wt. %	ND	ND	0.1	0.01	ND	ND	30	100
Sm	ppm	0.02	0.1	0.1	0.05	2000	2000	1000	10000
Sn	ppm	0.1	0.1	10	1	100	2000	10000	10000
Sr	ppm	0.5	1	10	2	2000	10000	5000	50000
Ta	ppm	0.05	0.1	0.5	0.1	2000	2000	10000	1000
Tb	ppm	0.02	0.1	0.05	0.01	2000	2000	1000	10000
Te	ppm	0.02	0.05	ND	ND	1000	1000	ND	ND
Th	ppm	0.1	0.1	0.1	0.2	2000	4000	1000	10000
Ti	wt. %	0.001	0.001	0.01	0.01	5	10	25	10
Tl	ppm	0.02	0.05	0.5	ND	1000	1000	1000	ND
Tm	ppm	0.02	0.1	0.05	0.01	2000	2000	1000	10000
U	ppm	0.1	0.1	2	0.1	2000	4000	10000	10000
V	ppm	1	2	10	8	10000	10000	50000	10000
W	ppm	0.1	0.1	5	0.5	100	200	10000	10000
Y	ppm	0.01	0.1	0.5	0.1	2000	2000	10000	50000
Yb	ppm	0.02	0.1	0.1	0.05	2000	2000	1000	10000
Zn	ppm	0.1	0.2	10	c	10000	10000	50000	ND
Zr	ppm	0.1	0.2	ND	5	2000	2000	ND	50000

ND not determined

Table 3. Comparison of Li concentrations (ppm) in till samples collected up-ice and down-ice of the North and South pegmatites. Refer to the master till sample map (Appendix B3) for sample locations. Till samples from the East Kemptville area (18CS series) are the average for Li determined by aqua regia/ICP-MS (Smith, 2019).

Sample	Interpretation	Distance down-ice from the deposit (m)	<0.063 mm fraction of till			1.0–2.0 mm fraction of till		
			Aqua regia	4-acid	Na-peroxide	Aqua regia	4-acid	Na-peroxide
East Kemptville Till (avg. of 18CS002, 007, 010, and 011)	Regional up-ice	-25000	22.5					
22MPB023	background up-ice	-1000	22.3	40.9	42.0	38.6	60.8	108.0
22MPB010	background up-ice	-100	18.6	30.4	32.0	27.6	52.1	104.0
22MPB035	down-ice S pegmatite	35	31.3	51.2	55.0	42.8	119.1	206.0
22MPB036	down-ice S pegmatite	50	47.5	65.9	67.0	55.8	80.3	126.0
22MPB009	down-ice N pegmatite	500	47.6	83.3	87.0	82.6	140.6	173.0
22MPB015	down-ice N&S pegmatites	2500	21.0	40.9	45.0	31.9	98.0	160.0
22MPB030	down-ice N&S pegmatites	5400	34.0	49.6	48.0	52.1	59.3	71.0
22MPB029	down-ice N&S pegmatites	8400	29.5	45.5	45.0	50.3	60.2	76.0
22MPB027	down-ice N&S pegmatites	13000	27.3	44.1	44.0	29.8	43.9	56.0

Upper Crust = 24 ppm indicates >90th percentile

S pegmatite = South pegmatite; N pegmatite = North pegmatite; N&S pegmatites = North and South pegmatites.

per beam. The samples were left in their original 4 dram polypropylene containers and covered with a 4 µm Prolene® film held in place by a small elastic band. The samples were turned upside down for analysis through the Prolene® film side and returned upright after analysis. Samples were repeated at the rate of 1 repeat every 10 samples (precision of analysis, homogeneity of samples). Data for the routine samples and quality assurance/quality control (QA-QC) samples analyzed using pXRF are reported in Appendix E.

RESULTS

Till geochemistry

The raw till geochemistry data files, as reported by the commercial laboratories, are presented in Appendix C, both as pdf files and Excel® files. GSC-formatted geochemical data are reported in Appendix D as Excel® files. Quality control data for field duplicates, laboratory (blind) duplicates, and certified reference materials that were added to the batches by the GSC lab are reported in Appendix H. Geochemical values determined using pXRF are reported in Appendix E and the pH values of selected samples are reported in Appendix C.

The 2020 data obtained by 4-acid digestion and aqua regia digestion were compared for three size fractions, 1.0–2.0 mm, <0.063 mm, and <0.002 mm (Brushett et al., 2022). Although the range of values for Li, Nb, Cs, and Ta was greater for the <0.002 mm fraction, the distribution of high and low values and spatial patterns were similar for all three size fractions.

To obtain a <0.002 mm fraction requires a larger bulk till sample (800 g versus only 100 g for a <0.063 mm fraction) be collected in order to recover sufficient clay-sized material for geochemical analysis. Also, sample preparation to recover the clay-sized fraction is more costly (~$40 per sample) and time consuming because it requires centrifuging. Due to the preliminary results and the greater costs and time required, the <0.002 mm fraction was not used in subsequent years as it provided no added benefit.

In 2021 and 2022, the 1.0–2.0 and <0.063 mm fractions were analyzed using three different analytical methods: Na-peroxide fusion, 4-acid digestion, and aqua regia digestion. A summary of the range of values for Li is reported in Table 3 and the range of values, mean, and threshold for potential LCT pegmatite pathfinder elements are listed in Table 4 for LCT pathfinder elements. Lithium distribution in the 1.0–2.0 mm and <0.063 mm fractions of till determined by the three different analytical methods are shown in Figure 14.

A total of 29 till samples were subjected to all three digestion methods for both size fractions. Some generalizations for Li concentrations can be made: 1) the <0.063 mm fraction contains a lower average concentration than its 1.0–2.0 mm counterpart; 2) the <0.063 mm fraction exhibits a lower standard deviation and variance than its 1.0–2.0 mm counterpart; and 3) aqua regia shows the lowest average concentration and Na-peroxide fusion shows the highest average concentration.

Strong linear correlations are evident for Li concentrations in the <0.063 mm fraction (Fig. 15): 1) aqua regia vs. Na-peroxide fusion $R^2 = 0.86$ (Fig. 15a); and 2) Na-peroxide fusion vs. 4-acid $R^2 = 0.95$ (Fig. 15b). Weaker correlations were found for the 1.0–2.0 mm fraction between 3) aqua regia vs. Na-peroxide fusion (Fig. 15c); and 4) Na-peroxide fusion vs. 4-acid (Fig.15d).

Table 4. Summary statistics for lithium-cesium-tantalum (LCT) pegmatite pathfinder elements in the <0.063 mm and the 1.0–2.0 mm till fractions. LOD = lower limit of detection. All values reported are in ppm.

Element and digestion method	LOD	<0.063 mm min	max	mean	threshold (90th percentile)	1.0–2.0 mm min	max	mean	threshold (90th percentile)
Li Na peroxide	10	17	127	45.4	65	37	531	109.1	163.5
Li 4-acid	0.1	16.5	97.7	39.5	53.2	31	140.6	61.2	98
Li aqua regia	0.1	9.9	88.4	27.8	40.2	10.3	85.5	37.7	56.4
Cs Na peroxide	0.1	1.6	17	4.4	6.6	2.4	25.5	4.8	7.7
Cs 4-acid	0.1	1.7	13	3.6	6.1	2.4	23.9	4.7	6.5
Cs aqua regia	0.02	0.4	11.1	2.4	4.4	0.4	19.4	2.8	5.6
Nb Na peroxide	2	6	163	22.7	34.7	7	66	19.6	34
Nb 4-acid	0.04	8.6	81.7	19.4	28.8	5.3	24.3	11.8	17.7
Nb aqua regia	0.02	0.02	16.3	1.0	1.63	0.1	3.3	0.4	0.67
Ta Na peroxide	0.5	0.7	10.5	1.7	2.4	0.5	5.7	1.3	1.7
Ta 4-acid	0.1	0.6	4.6	1.4	2.2	0.4	4.4	1.0	2.1
Ta aqua regia	0.05	<LOD	<LOD	<LOD		<LOD	<LOD	<LOD	
Be Na peroxide	5	2.5	7	2.5	2.5	5	9	6.8	8.8
Be 4-acid	1	1	7	2.2	3	1	4	2.2	4
Be aqua regia	0.1	0.1	1.2	0.4	0.6	0.1	1.6	0.4	0.6
P Na peroxide	100	300	3700	880	1200	200	2600	570	850
P 4-acid	10	230	1860	820	1250	150	1080	460	760
P aqua regia	10	100	3820	800	1150	140	2410	520	820
Ti Na peroxide	100	4700	19500	8640	11340	2600	18100	5230	7400
Ti 4-acid	10	3890	14090	7530	11830	1990	7360	3920	5690
Ti aqua regia	10	240	2360	690	1020	60	1740	890	1410
W Na peroxide	5	<LOD	2.5		2.5	<LOD	7		7
W 4-acid	0.1	0.7	3.9	1.5	2.0	0.6	1.5	0.9	1.4
W aqua regia	0.1	0.1	1.7	0.2	0.4	0.1	1.5	0.2	0.2
Th Na peroxide	0.1	4.7	30.3	13.7	21.9	4.9	13.6	7.5	9.5
Th 4-acid	0.1	5.9	35.7	13.3	21.2	5.2	9.7	6.6	8.7
Th aqua regia	0.1	0.7	15.8	7	10.2	3.5	10.6	5.7	6.7

When comparing size fractions (Fig. 16): 1) aqua regia <0.063 mm vs. 1.0–2.0 mm $R^2 = 0.51$ (Fig 16a); 2) 4-acid <0.063 mm vs. 1.0–2.0 mm $R^2 = 0.63$ (Fig 16b); and 3) Na-peroxide fusion <0.063 mm vs. 1.0–2.0 mm $R^2 = 0.26$ (Fig 16c).

Log-normalized correlation matrices are presented for the three digestion methods and both size fractions (Appendix F). R^2 values >0.7 are considered to indicate a strong correlation with Li (*see* Discussion *below*).

A strong correlation exists between Li and Mg for the <0.063 mm fraction analyzed by aqua regia; however, the origin of this correlation, though unclear, likely reflects chlorite alteration of the metavolcanic host rocks surrounding the Brazil Lake pegmatite. Alternatively, it may also reflect the presence of a tourmaline alteration shell around the pegmatites, although aqua regia digestion is not likely strong enough to dissolve any significant quantity of tourmaline. Additional strong positive correlations exist for the 1.0–2.0 mm fraction analyzed by aqua regia, including those between Li and Al, K, Fe, and Ga. Magnesium and Fe association with Li suggest that Li may related to chlorite and/or tourmaline (as discussed above), though Al, K, and Ga associations with Li could indicate a link with muscovite. However, Al and Ga concentrations could also reflect contributions from spodumene.

In the <0.063 mm fraction, there is a strong correlation between Li and Cs when determined by 4-acid. This reflects the dispersal of spodumene and/or Cs-rich muscovite. The weak negative correlation between Li and Na determined by 4-acid digestion indicates that the source of the Li is not pollucite $[(Cs,Na)_2(Al_2Si_4O_{12})\cdot 2H_2O]$. Varying correlations exist between Li and Cr, Cs, Fe, Mg, Sc, Sr, V, Ti, and Ta for the 1.0–2.0 mm fraction analyzed by 4-acid. Elevated Cr, Fe, and Mg concentrations reflect the presence of chlorite, and Cs, Sc, Ti, V, and Ta reflect the presence of oxides.

There is a strong correlation between Li and Cs for the <0.063 mm fraction determined by Na-peroxide fusion. This reflects the dispersal of spodumene and/or

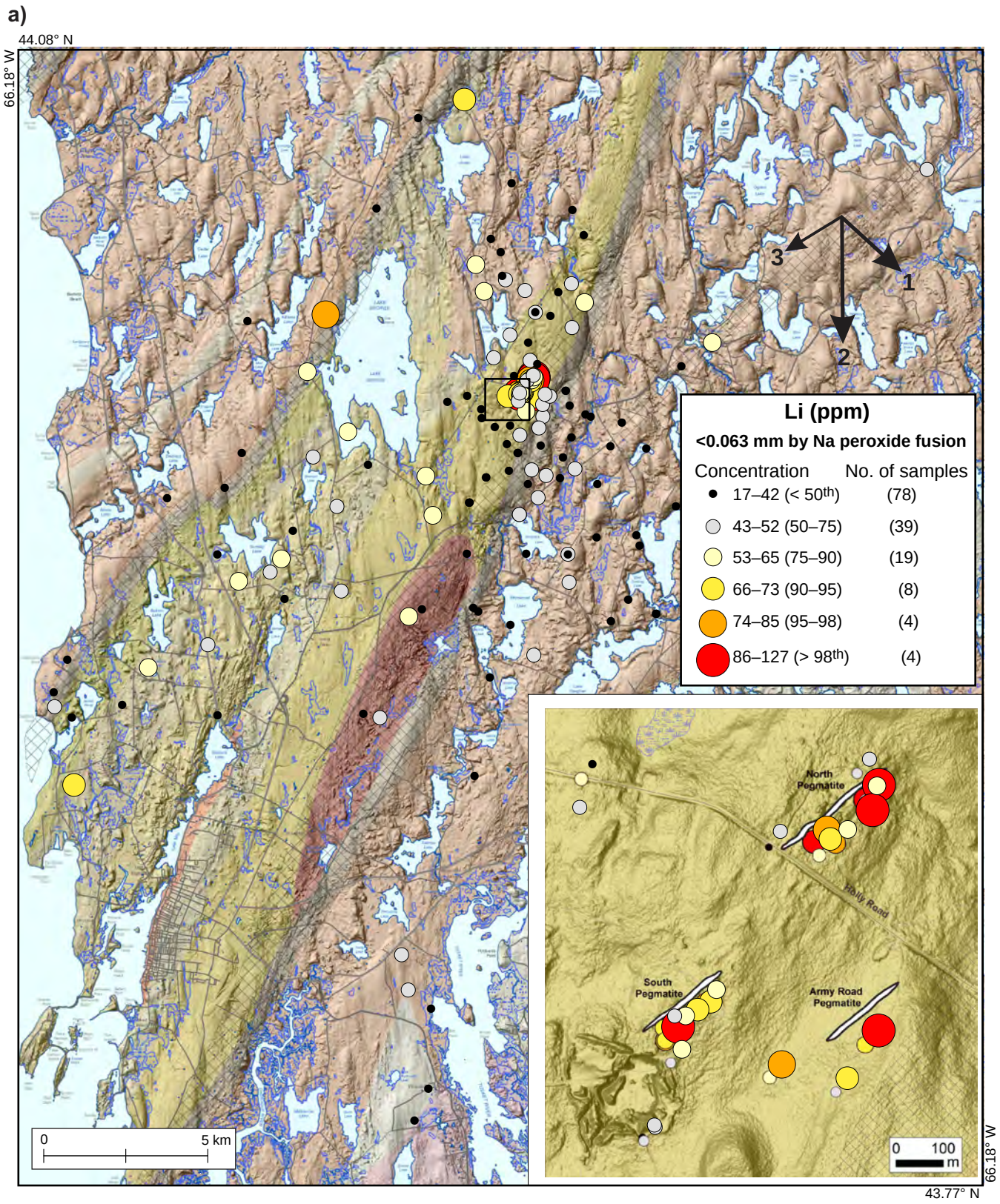

Figure 14. Proportional dot maps of Li concentrations in till. Bedrock geology legend is shown in Figure 2. Generalized ice-flow phases are shown by arrows and their relative ages, based on regional ice-flow history by Stea and Grant (1982) and Finck and Stea (1995), are indicated by numbers, with one being the oldest. **a)** <0.063 mm till fraction analyzed using Na-peroxide fusion followed by ICP-MS, n=152.

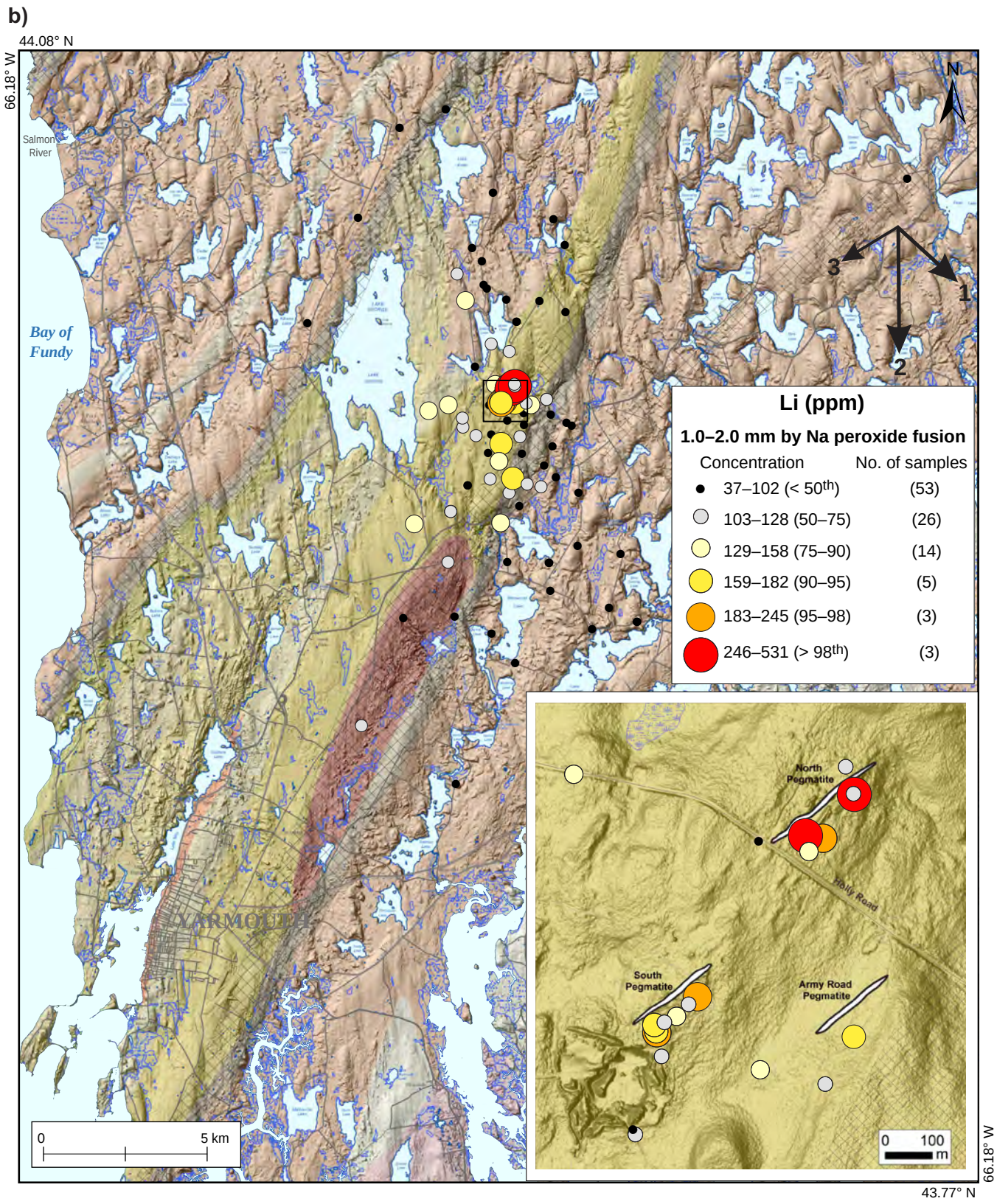

Figure 14 continued. Proportional dot map of Li concentrations in till. Bedrock geology legend is shown in Figure 2. Generalized ice-flow phases are shown by arrows and their relative ages, based on regional ice-flow history by Stea and Grant (1982) and Finck and Stea (1995), are indicated by numbers, with one being the oldest. **b)** The 1.0–2.0 mm till fraction analyzed using Na-peroxide fusion followed by ICP-MS, n=104.

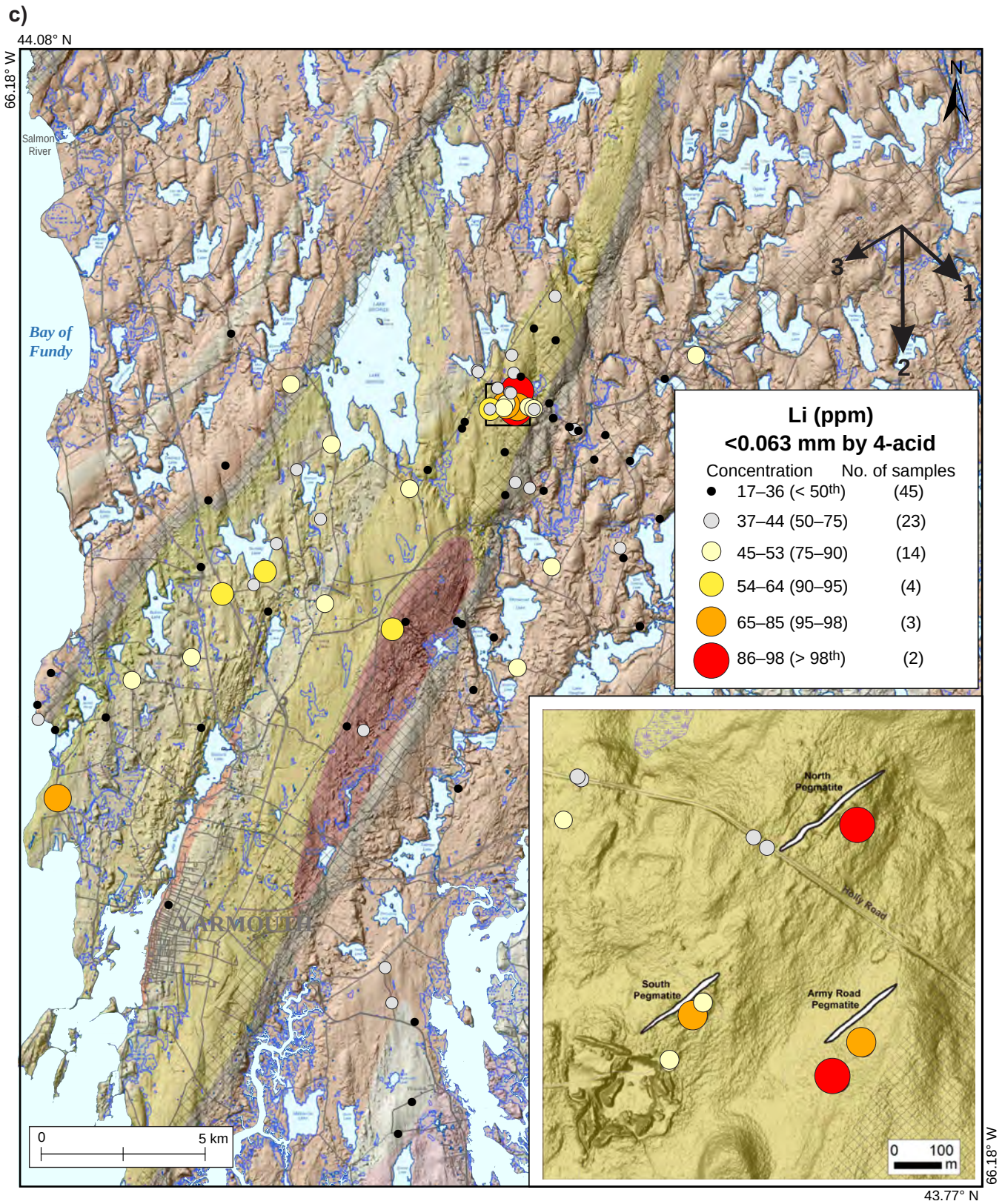

Figure 14 continued. Proportional dot map of Li concentrations in till. Bedrock geology legend is shown in Figure 2. Generalized ice-flow phases are shown by arrows and their relative ages, based on regional ice-flow history by Stea and Grant (1982) and Finck and Stea (1995), are indicated by numbers, with one being the oldest. **c)** The <0.063 mm till fraction analyzed using 4-acid digestion followed by ICP-MS, n=91.

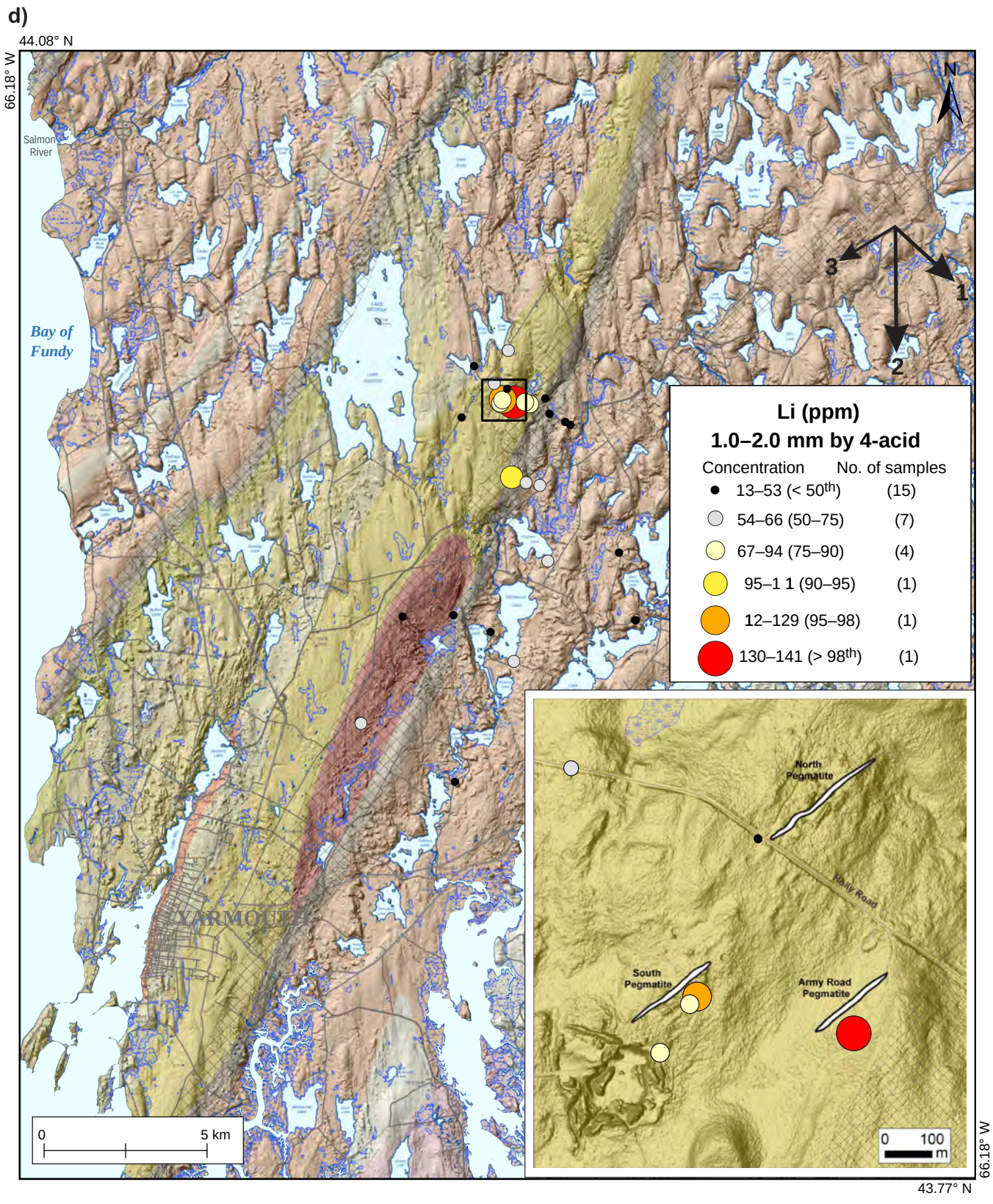

Figure 14 continued. Proportional dot map of Li concentrations in till. Bedrock geology legend is shown in Figure 2. Generalized ice-flow phases are shown by arrows and their relative ages, based on regional ice-flow history by Stea and Grant (1982) and Finck and Stea (1995), are indicated by numbers, with one being the oldest. **d)** The 1.0–2.0 mm till fraction analyzed using 4-acid digestion followed by ICP-MS, n=29.

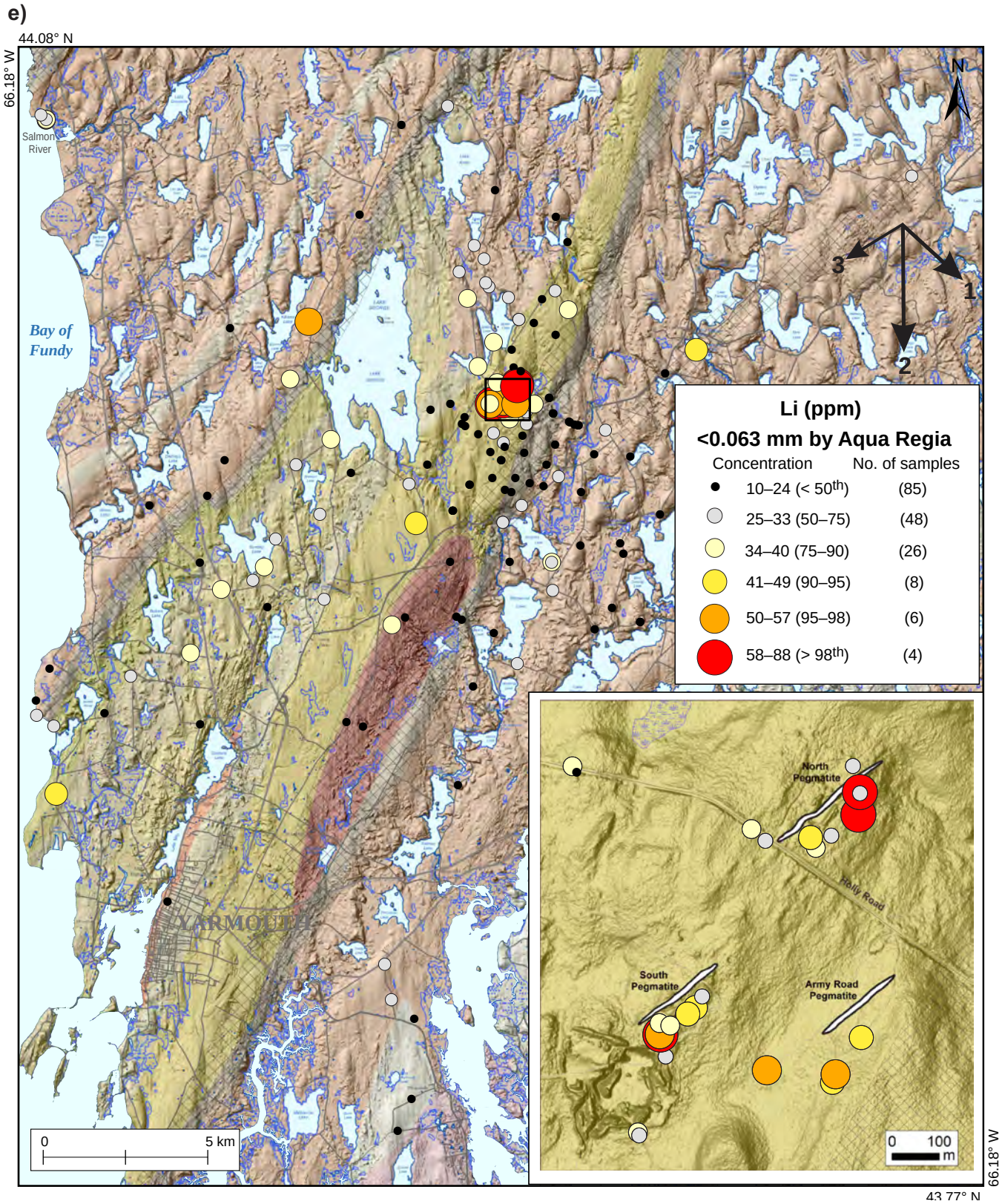

Figure 14 continued. Proportional dot map of Li concentrations in till. Bedrock geology legend is shown in Figure 2. Generalized ice-flow phases are shown by arrows and their relative ages, based on regional ice-flow history by Stea and Grant (1982) and Finck and Stea (1995), are indicated by numbers, with one being the oldest. **e)** The <0.063 mm till fraction analyzed by aqua regia followed by ICP-MS, n=177.

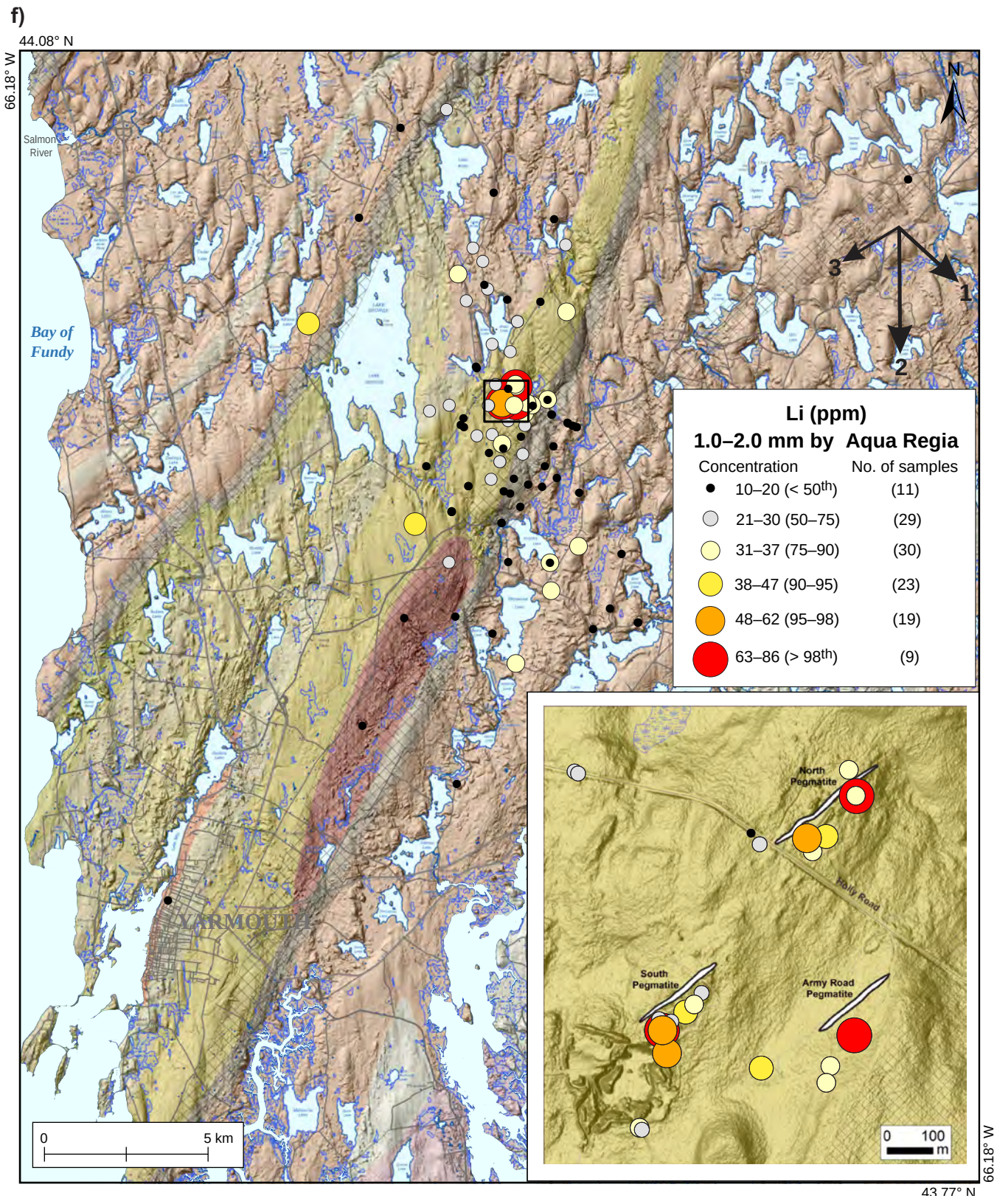

Figure 14 continued. Proportional dot map of Li concentrations in till. Bedrock geology legend is shown in Figure 2. Generalized ice-flow phases are shown by arrows and their relative ages, based on regional ice-flow history by Stea and Grant (1982) and Finck and Stea (1995), are indicated by numbers, with one being the oldest. **f)** The 1.0–2.0 mm till fraction analyzed using aqua regia digestion followed by ICP-MS, n=121.

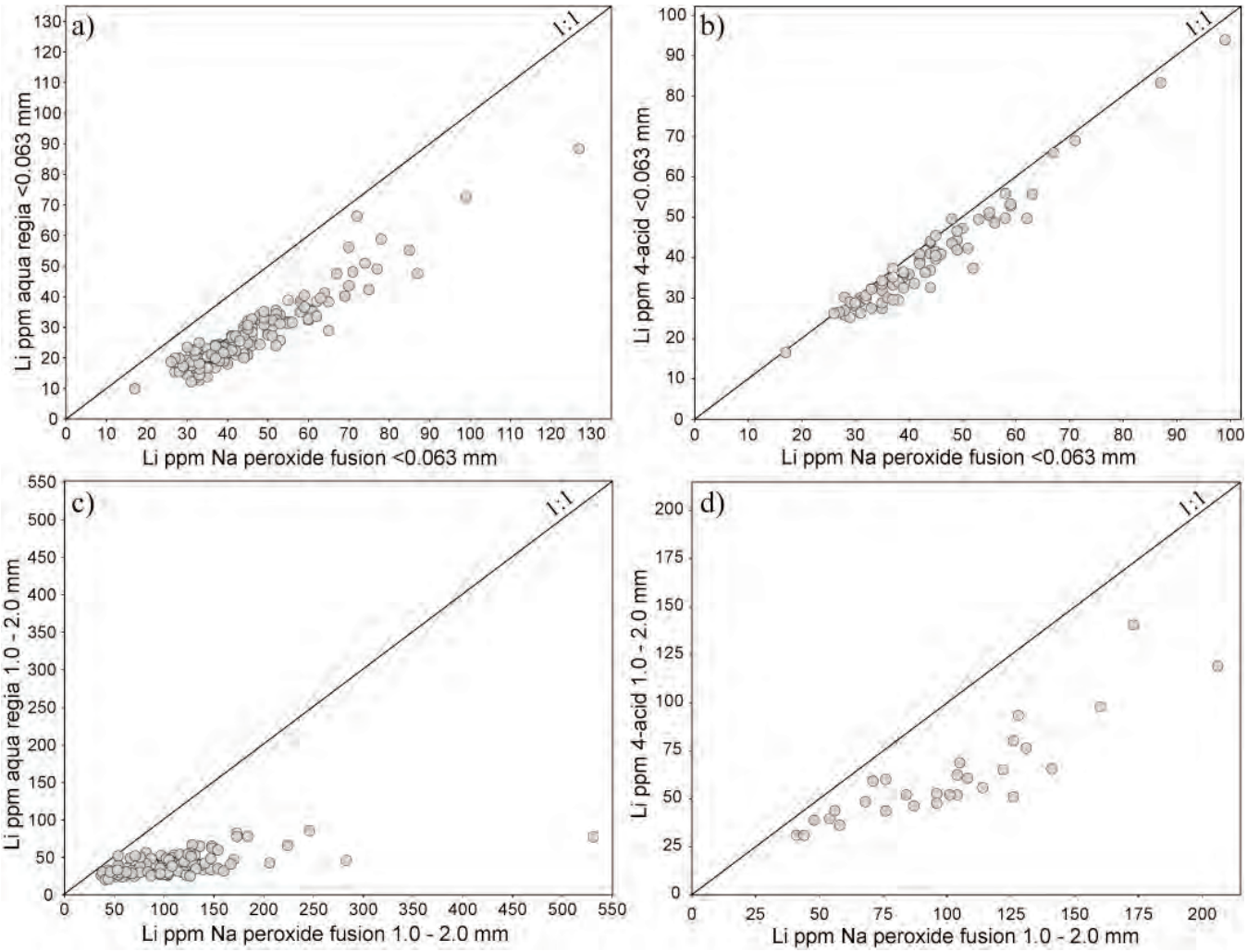

Figure 15. Scatter plots comparing the three digestion methods to their size fraction counterparts (samples from 2020–2022). Concentrations of Li (ppm) in <0.063 mm fraction determined by Na-peroxide fusion versus Li concentrations determined by **(a)** aqua regia (n=152) and by **(b)** 4-acid (n=74). Concentrations of Li (ppm) in the 1.0–2.0 mm fraction determined by Na-peroxide fusion versus Li concentrations determined by **(c)** aqua regia (n=104) and by **(d)** 4-acid (n=29).

Cs-rich muscovite, similar to the correlation noted above for the 4-acid results of the fine fraction. Correlations between Li and Ga reflect the presence of spodumene in association with feldspar and mica as well as sphalerite.

Portable XRF analysis was completed on the 22MPB sample set (Appendix E). Although Li cannot be analyzed via pXRF, this method does allow for the detection of other Li pegmatite pathfinder elements such as Ti, Zn, Sr, and Th (Fig. 17). Based on poor correlation with the Na-peroxide fusion results and poor precision reported for replicates and duplicates (Appendix E1), the pXRF results for elements such as P and Sn are considered to be unreliable.

Till geochemistry spatial patterns

Proportional dot maps of selected elements are included in Appendix G and selected maps for Li are shown in Figure 14. Data classes for each dot size were determined using percentiles calculated in ArcMap (v. 10.8.1). For sites where multiple till samples were collected, only the uppermost sample or the first sample of a field duplicate pair were plotted on the maps. Values reported as less than detection limit were reassigned values of 1/2 the lower detection limit prior to plotting. Pathfinder elements for LCT pegmatites have previously been identified (Černý, 1991; Černý and Ercit, 2005; Steiner, 2019), including the most commonly Li, Cs, and Ta, but Be, B, Co, Rb, Zr, Nb, Sn, and W can also be included. Maps were made for these 11 elements (Fig. 14 and Appendix G).

Figure 15 shows that the Li values from various methods and fractions all exhibit acceptable positive correlations, indicating that any of these methods can potentially be used for exploration. However, for the 1–2 mm fraction, aqua regia is the least reliable method for determining Li concentration.

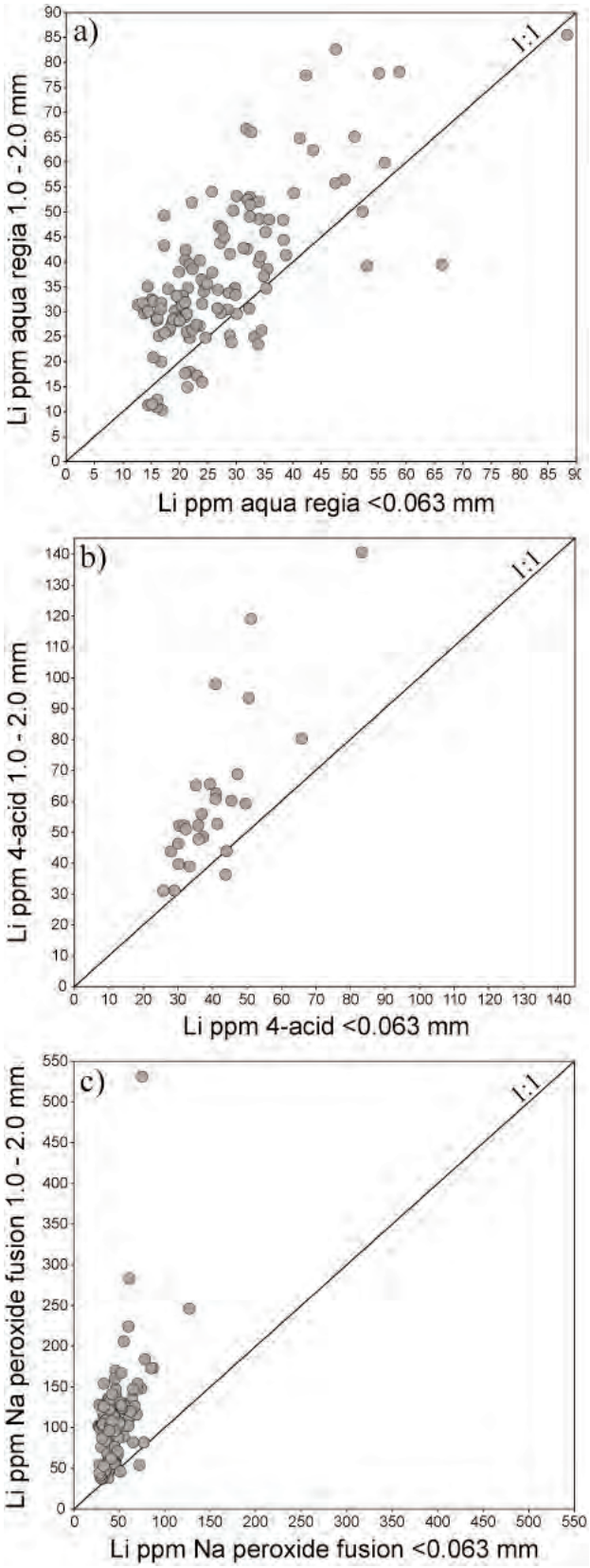

Figure 16. Scatter plots comparing the concentrations of Li (ppm) in the 1–2 mm fraction and the <0.063 mm fraction determined by **(a)** aqua regia (n=104), **(b)** 4-acid (n=28), and **(c)** Na-peroxide fusion (n=121) for samples collected in 2020 through 2022.

Overall, the location of the Brazil Lake pegmatites can be identified using any of the three types of analyses Note that Li concentrations in numerous samples collected down-ice of the deposit are within the 90th percentile or higher. Sodium peroxide fusion results for the <0.063 mm fraction (Fig. 14a) show a strong (90 to 98th) percentile anomaly immediately (0–200 m) down-ice of the Brazil Lake and Army Road pegmatites. Lithium concentrations in samples collected farther down-ice (from 0.5–5 km) generally are in the <75th percentile. Background samples up-ice of the Brazil Lake pegmatites contain Li values up to the 90th percentile, most notably west of Lake George and north of Lake Annis, which was unexpected. Sodium peroxide fusion results for Li in the 1.0–2.0 mm fraction (Fig. 14b) show a strong (>90th percentile) positive anomaly directly over the deposit with samples down-ice (south), outlining a narrow 3 km dispersal train of Li values between the 75th and 95th percentiles. This down-ice dispersal pattern is not apparent for the other analytical methods or size fractions discussed above. The 1.0–2.0 mm fraction of till samples collected to the southwest were not analyzed by Na-peroxide fusion, thus any anomalies to the southwest cannot be evaluated using this analytical method. Results for other Li pegmatite pathfinder elements (Černý and Ercit, 2005) obtained by Na-peroxide fusion from the <0.063 mm fractions are discussed below. No noteworthy differences were observed among the analyses.

The Li results from the 4-acid digestion of the <0.063 mm fraction (Fig. 14c) reveal a strong (>75th percentile) anomaly immediately down-ice of the Brazil Lake pegmatites with other samples further down-ice (from 0.5–5 km) primarily in the <75th percentile. The southwest linear dispersal as noted above is also present for the 4-acid results. The Li results of the 1.0–2.0 mm fraction analyzed by 4-acid digestion (Fig. 14d), though limited to a small dataset, reflect a similar pattern to that of the results of the <0.063 mm fraction also determined by 4-acid (minus the southwest linear dispersal).

The Li values for the <0.063 mm fraction measured by aqua regia (Fig.14e) show a strong positive anomaly (>95th percentile) immediately down-ice (south) 0–-200 m of the deposit but the anomaly quickly disappears further down-ice to the south (at 0.5–5 km), with samples plotting primarily in the <50th percentile. The area interpreted to be background (up-ice of Brazil Lake pegmatites) at the time of the sampling displays higher concentrations of Li than the samples down-ice of the Brazil Lake pegmatites. There is also a linear >75th percentile anomaly trending to the southwest of Brazil Lake pegmatites, between the Cranberry Point shear zone and the Chebogue Point shear zone. This trend parallels the 3rd ice-flow direction to the south-

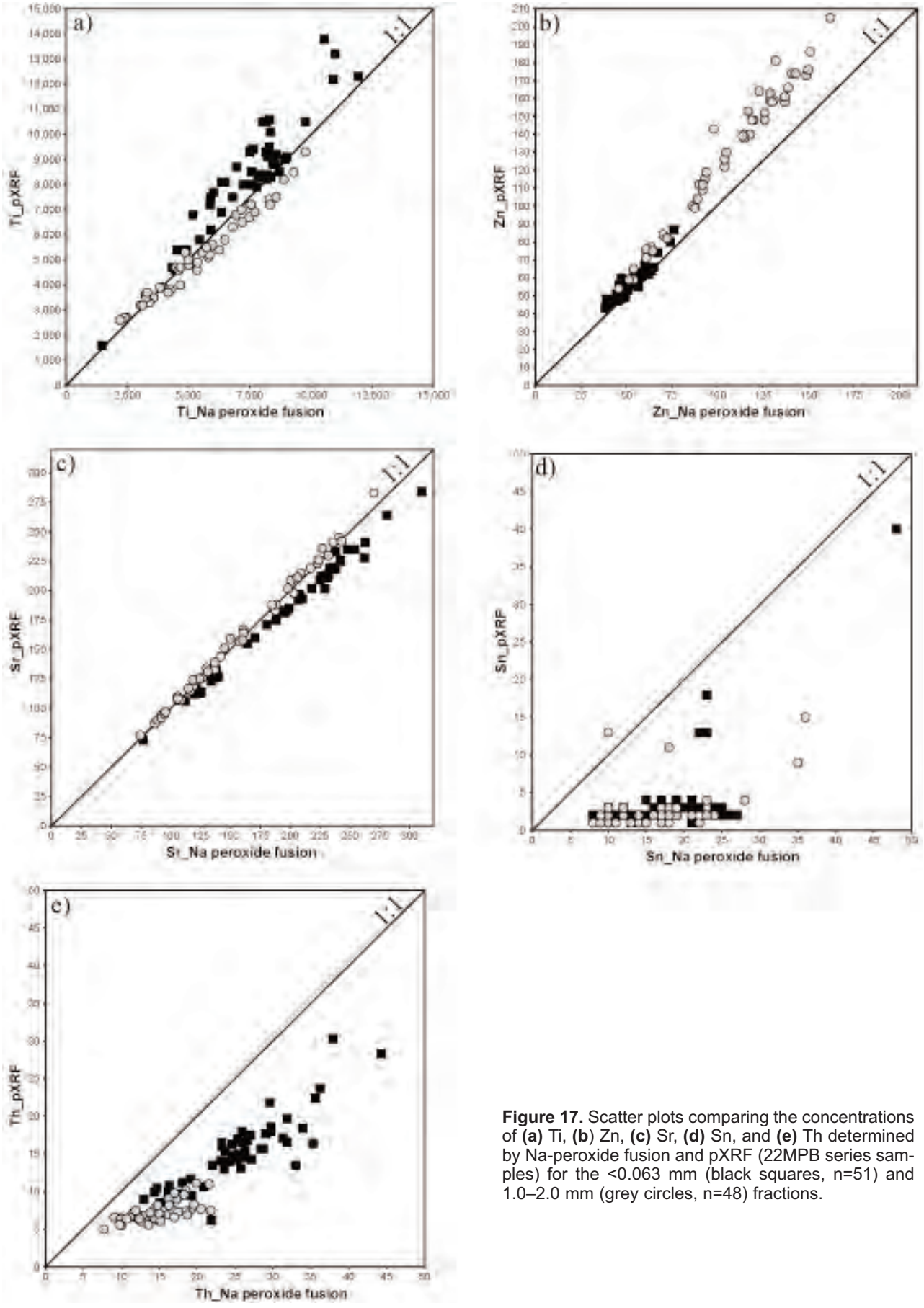

Figure 17. Scatter plots comparing the concentrations of **(a)** Ti, **(b**) Zn, **(c)** Sr, **(d)** Sn, and **(e)** Th determined by Na-peroxide fusion and pXRF (22MPB series samples) for the <0.063 mm (black squares, n=51) and 1.0–2.0 mm (grey circles, n=48) fractions.

west. Li values determined by aqua regia digestion of the 1.0–2.0 mm fraction (Fig.14f) show a very similar pattern, with the exception that the down-ice (southward) samples are plotting in the 50th to 75th percentile, in contrast to the <50th percentile for the fine fraction as noted above.

Cesium exhibits a strong >75th percentile anomaly immediately down-ice of the North, South and Army Road pegmatites, with values highest south and southwest of the Army Road pegmatite. Cesium values between the 75th and 95th percentiles were found up-ice of the three pegmatites and on all sides of Brazil Lake. Notably, there is no distinguishable down-ice dispersal of Cs more than 200 m from the pegmatites (*see* Appendix G, maps 1–4).

Tantalum has no distinguishable anomaly immediately down-ice of the Brazil Lake pegmatites but does have concentrations in the >75th percentile up to 20 km (the limit of sampling) to the south and southwest of the South pegmatite. Other notably elevated Ta values occur just south of the Army Road pegmatite, to the west of the South pegmatite, north of Lake Annis, south of Sunday Lake, and southeast of Island Pond (*see* Appendix G, maps 5–8).

Beryllium concentrations are mostly below detection limit when analyzed by Na-peroxide fusion or by aqua regia using the <0.063 mm and 1.0–2.0 mm fractions. Exceptions are the few above detection limit values for 1.0–2.0 mm fraction analyzed by Na-peroxide (*see* Appendix G, map 9).

Rubidium concentrations just down-ice of the Brazil Lake pegmatites are low and primarily below the 75th percentile. Values for Rb are elevated (90–95th percentile) south and southwest of the Army Road pegmatite. Rubidium concentrations directly up-ice are between the 75th and 95th percentile, with notably high values surrounding Brazil Lake and just south of the village of Carleton (*see* Appendix G, maps 10–13).

Niobium concentrations just down-ice of the Brazil Lake pegmatites are low, primarily less than the 75th percentile. Samples collected >500 m down-ice of the Brazil Lake pegmatites have Nb concentrations generally greater than the 75th percentile (*see* Appendix G, maps 15–18).

Tin concentrations just down-ice of the Brazil Lake pegmatites are low (<75th percentile), though they are elevated southwest of the pegmatites, between the two shear zones. Just south of the Army Road pegmatite, Sn concentrations are between the 90th and 95th percentiles (*see* Appendix G, maps 19 and 20).

Although there is significant tourmaline enveloping the deposit, B concentrations are at or below limit of detection for the each of the analytical methods (no map shown). Zirconium concentrations in the till are low and do not show any relationship to the three pegmatites (*see* Appendix G, map 14). Tungsten concentrations (4-acid data only) just down-ice of the Brazil Lake pegmatites are low (<75th percentile) and no clear dispersal pattern is evident (*see* Appendix G, maps 21 and 22).

In summary, Ta, Be, Rb, Nb, Sn, and Li concentrations are highest just south of the Brazil Lake pegmatites and to the southwest, between the Cranberry Point and the Chebogue Point shear zones.

DISCUSSION

The aims of this study were to investigate effective methods for Li exploration in glaciated terrain, and to identify cost effective methods for exploration. Na-peroxide fusion, which is a total digestion for Li minerals (Yu et al., 2007; de Souza et al., 2022), and as such, discussion here will compare the two additional analytical methods (aqua regia and 4-acid) to Na-peroxide fusion to determine if aqua regia and/or 4-acid are also suitable for Li exploration, or if Na-peroxide fusion should be the preferred method.

Size fraction comparison

Two size fractions were investigated in this study: 1) the <0.063 mm fraction, which is the traditional size fraction used for till geochemistry analyses (McClenaghan et al., 2023a, b) and 2) the 1.0–2.0 mm fraction. Both size fractions were investigated because spodumene is a relatively robust silicate with a high Mohs hardness of 6.5–7, which means that it could be abundant in the coarse fraction of the till.

The background Li content in the local till is sourced from minerals containing Li as an accessory element, most commonly in mica or clay minerals (i.e. sheet silicates or phyllosilicate minerals). Mica and clay minerals are considerably more susceptible to physical and chemical degradation than spodumene and would be preferentially concentrated in the fine (<0.063 mm) fraction. One challenge of investigating the coarse fraction of till is the potential for "nugget" effects of spodumene crystals. This effect is reflected in the generally higher standard deviation and variance of the coarse-fraction relative to the fine-fraction using the three digestion methods investigated (Table 5). Overwhelmingly, Li concentrations are consistently higher in the 1.0–2.0 mm fraction than in the <0.063 mm fraction: aqua regia = 21.42%, 4-acid = 29.33%, and Na-peroxide fusion = 50.82% on average, which confirms the proposed hypothesis.

Comparison of Na-peroxide fusion and aqua regia digestion

Aqua regia

Aqua regia is a long standing and commonly used partial to near total (depending on the element and mineral

Table 5. Comparison of lithium statistics for the three digestion methods and two size fractions used in this study.

Digestion method	Size fraction (mm)	Number of analyses	Minimum (ppm)	Maximum (ppm)	Mean (ppm)	Median (ppm)	Standard deviation
Na-peroxide fusion	<0.063	152	17.0	127.0	45.4	42.0	15.3
Na-peroxide fusion	1.0–2.0	104	37.0	531.0	109.1	102.0	61.1
4-acid	<0.063	91	16.5	97.7	39.3	36.0	13.9
4-acid	1.0–2.0	29	31.0	140.6	61.2	52.7	25.2
Aqua regia	<0.063	177	9.9	88.4	27.8	24.4	11.4
Aqua regia	1.0–2.0	121	10.3	85.5	37.7	34.4	15.2

phase) digestion (of unconsolidated sediments) used for the exploration of base metals and gold (Marsden and House, 2006; McClenaghan et al., 2023c). But is it also an appropriate digestion method of till for Li-pegmatite exploration? A binary plot comparing the values obtained from the fine-fraction using Na-peroxide fusion and aqua regia (Fig. 15a) shows a strong correlation ($R^2 = 0.86$), but with aqua regia values generally around 60% of the total Na-peroxide values (Appendix D6). The lower aqua regia values indicate that this method cannot effectively digest all the Li-bearing phases. Although aqua regia does not provide a total digestion of Li-bearing minerals, the strong linear correlation of the results for the two digestion methods does suggest that either method is suitable for vectoring studies. Perhaps a correction factor could be applied to the aqua regia data to estimate a total Li value; however, this would need to be studied further to assess the impact of varying mineralogy on the difference between the 2 digestion methods.

A comparison of the results for the coarse fraction using Na-peroxide fusion and aqua regia (Fig. 15c) shows a weak correlation ($R^2 = 0.35$) that greatly deviates from the 1:1 line (slope = 0.14). This plot shows that an aqua regia partial digest cannot effectively digest the coarse fraction, where it is suspected that the bulk of the Li is contained in spodumene. Aqua regia values for the 1–2 mm fraction varies between 16 and 96% of the total value, but on average are only 40% of the total concentration. For analyses of the coarse fraction, aqua regia is inferior to the Na-peroxide fusion method in its ability to digest the dominant Li-bearing phases.

Comparison of Na-peroxide fusion and 4-acid digestion

4-acid digestion

Four-acid digestion is a near-total digestion method used for extracting elements from resistant minerals, primarily for lithogeochemical applications (Chao and Sanzolone, 1992). Is it also suitable for analyzing till samples for Li-pegmatite exploration? A binary plot comparing the results of the fine fraction using Na-peroxide fusion and 4-acid (Fig. 15b) shows a nearly 1:1 correlation ($R^2 = 0.95$, slope 0.92). This pattern indicates that there is almost no difference in the ability of 4-acid to digest all the Li-bearing material in the sample versus Na-peroxide fusion. A comparison of the coarse fraction results between Na-peroxide fusion and 4-acid (Fig. 15d) shows a moderate correlation ($R^2 = 0.77$). The deviation from the 1:1 line (slope =0.56), increases with increasing Li concentration. This pattern shows that 4-acid digestion is not as robust as Na-peroxide fusion, particularly at higher Li (>100 ppm) concentrations but is significantly better than aqua regia. Thus, 4-acid is an effective and acceptable method for the digestion of the fine fraction. For analyses of the coarser fraction, however, 4-acid digestion is less effective compared to Na-peroxide fusion in its ability to dissolve the dominant Li-bearing phases in this fraction.

Sodium peroxide fusion

Sodium peroxide fusion analyses provide the most complete digestion and representation of the "total" Li concentration of a sample (Yu et al., 2007; de Souza et al., 2022). But is Na-peroxide fusion worth the extra cost? Like any method, Na-peroxide fusion has its strengths and weaknesses. It is the optimal commercial method for determining the total Li content as well as the content of other metals associated with LCT pegmatites (i.e. Cs and Ta). One of the challenges of this method is its higher limits of detection (e.g. Li 10 ppm) compared to 4-acid digestion (e.g. Li 0.1 ppm) or aqua regia digestion (e.g. Li 0.1 ppm) for Li, Cs, Ta, and other elements. The ability of Na-peroxide fusion to provide a total abundance of Li, despite the higher LOD, with higher precision, relative to any of the other analysis types, is a benefit as it can effectively identify the dispersal train of a feature that is as small as a pegmatite dyke only a few metres wide. Figure 18 emphasizes this point, showing the total Li concentrations (determined by Na-peroxide fusion) minus the partial Li content determined by aqua regia. However, disadvantages of the Na-peroxide fusion method include the requirement of a significantly larger aliquot compared

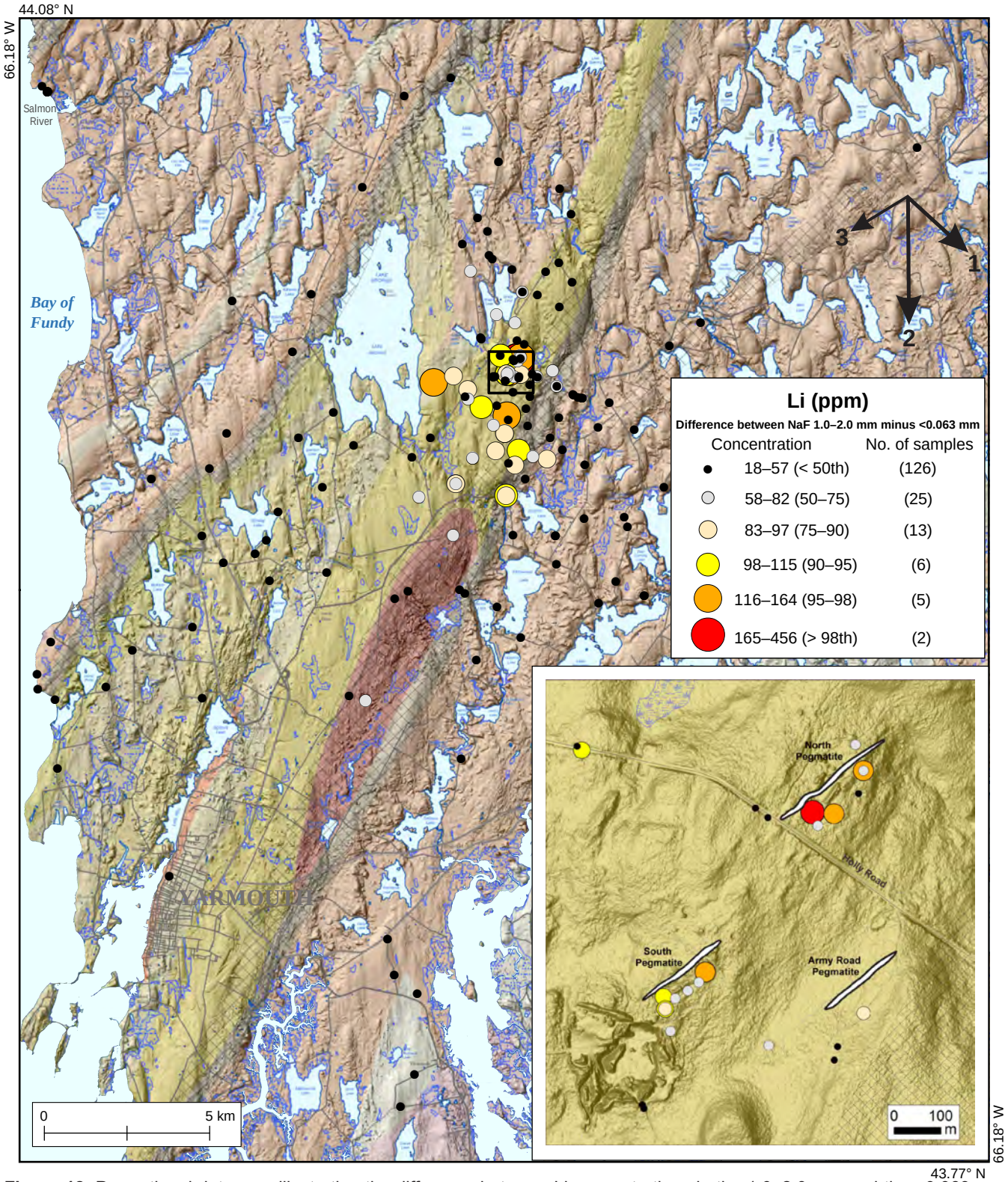

Figure 18. Proportional dot maps illustrating the difference between Li concentrations in the 1.0–2.0 mm and the <0.063 mm fractions analyzed by Na-peroxide fusion. Bedrock geology legend is shown in Figure 2. Generalized ice-flow phases are shown by arrows and their relative ages, based on regional ice-flow history by Stea and Grant (1982) and Finck and Stea (1995), are indicated by numbers, with one being the oldest.

Table 6. Cost comparison for aqua regia, Na-peroxide fusion and 4-acid digestion methods for the <0.063 mm and 1.0–2.0 mm fractions.

Digestion method	Size fraction	Sample sieving	Pulverize (agate mill)	Digestion and analyses	Total cost
Aqua regia	<0.063 mm	$5.00	NA	$42.00	$47.00
Aqua regia	1.0–2.0 mm	$5.00	$6.00	$42.00	$53.00
Na-peroxide fusion (54 elements)	<0.063 mm	$5.00	NA	$42.00	$47.00
Na-peroxide fusion (54 elements)	1.0–2.0 mm	$5.00	$6.00	$42.00	$53.00
4-acid	<0.063 mm	$5.00	NA	$50.00	$55.00
4-acid	1.0–2.0 mm	$5.00	$6.00	$50.00	$61.00

the other methods (5.0 g versus 0.5 g) as well as a higher cost per sample (Table 6).

Brazil Lake dispersal train

In general, the threshold between background and anomalous concentrations of elements in till is dependent on the regional up-ice bedrock geology, size of the mineral occurrence, erosional history, number of ice flows, mineral comminution, and the concentration of the elements in the bedrock source. During greenfield exploration, when mineralization is unknown, probability plots can be used to determine the threshold between background and anomalous concentrations. For case studies such as this one, where mineralization is known, a threshold between background and anomalous values can be determined by investigating samples up-ice and down-ice of the known mineralization to determine an appropriate threshold (Table 3). The most effective method for identifying the Brazil Lake pegmatites glacial dispersal in till, as noted above, is by using a Na-peroxide fusion on the 1.0–2.0 mm fraction. The net pattern of glacial dispersal from both the North and South pegmatites is detectable up to 4 km to the south of the North pegmatite using till geochemistry (Fig. 14b, 18).

There are differences in the trace element signatures of till samples immediately down-ice (50-200 m) of the three pegmatites (*see* Table 7 for a summary of the anomalous elements (>90th percentile) in specific areas). Till just down-ice of the North and South pegmatites is enriched in Li, Be, Cs, Nb, Rb, Ta, and W. Till south of the Army Road pegmatite is characterized by elevated values of Li, Cs, Rb, Sn, and Ta.

Comparison to other studies

Over the past 60 years, exploration for LCT pegmatites in glaciated terrain has been initiated and guided by the presence of pegmatite boulders (e.g. Schultz, 1971; Nikarinnen and Björklund, 1975; Steiger, 1977; Sarappää et al., 2015; Barros et al., 2022), including those found around the Brazil Lake pegmatites. In contrast to commodities such as Cu, Pb, Zn, and Au (e.g. McClenaghan and Paulen, 2018 and references therein), only a few case studies have been conducted to evaluate the effectiveness of till geochemistry for Li exploration (Table 8). These include those reported by Toverud (1987), Nikkarinen and Björklund (1975), Ahtola et al. (2015) and studies around the Brazil Lake pegmatites (Lundrigan 2008; MacDonald et al. 1992). Exploration programs, such as those reported by Li-FT Power (2022), demonstrate the value of till geochemistry for Li exploration. And recently, regional till geochemical data sets have been included in assessments of Li potential in key regions (e.g. Ahtola et al., 2015; Rasilainen et al., 2018; Chudasama and Sarala, 2022; Rossiter, 2023).

For all these studies and regional surveys, the highest Li values are summarized in Table 8 to allow for comparison with results of the Brazil Lake study. In our study, the highest Li values in till were determined using a Na-peroxide fusion and by analyzing the sand-sized fraction (1–2 mm). Other studies have reported a range of Li values determined by Na-peroxide fusion, 4-acid, or aqua regia methods. The size fractions that were analyzed range from <0.063 mm to fine to coarse sand. The reported Li concentrations in till proximal to Li-rich pegmatites range from 100s to 1000s of ppm (Table 8). Similar to this study, the Geological Survey of Finland determined total Li content in till using Na-peroxide fusion (e.g. Ahtola et al., 2015; Kontoniemi, 2011, 2012, 2013). The highest Li values reported in till in the studies in Finland are from the Kaustinen region in western Finland, a significant Li province in the European Union (Ahtola et al., 2015).

Future work

This GSC publication is the first of two GSC reports to publish data from the Brazil Lake till study. The second report will describe the indicator mineral results for bedrock samples and for till samples collected around the pegmatites. Examination of the pebble fraction of the till samples is underway and will be reported at a later date. Lithium isotope signatures will be determined for selected bedrock and indicator minerals from the Brazil Lake pegmatites. Stratigraphic studies are also currently in progress to provide a better understanding of the glacial history and stratigraphic context of the depositional record of western Nova Scotia.

All geochemical results described in this report were from B and C-horizon till samples; further work will include a comparison of B and C horizon samples to improve the understanding of how spodumene breaks down during glacial transport and how the geochemical response varies between them.

Table 7. Listing of pathfinder elements that display anomalous concentrations around the Brazil Lake pegmatites, the Army Road pegmatite, and other locations in the study area. (BLP = Brazil Lake pegmatites; NA = not applicable)

Element	Size fraction (mm)	Analytical method	North pegmatite	South pegmatite	Army Road pegmatite	Shear Zone	South of BLP	North of BLP	near Lake Annis	Appendix G map
Be	1–2	Na-peroxide	yes	no	no	yes	yes	no	NA	Map 9
Cs	<0.063	Na-peroxide	yes	yes	yes	no	no	yes	no	Map 1
	<0.063	4-acid	yes	yes	yes	no	no	no	no	Map 3
	1–2	Na-peroxide	yes	yes	yes	no	no	no	no	Map 2
	1–2	4-acid	no	yes	yes	no	yes	no	no	Map 4
Li	<0.063	Na-peroxide	yes	yes	yes	no	no	no	yes	Figure 14a
	<0.063	4-acid	yes	yes	yes	yes	no	NA	NA	Figure 14c
	<0.063	aqua regia	yes	yes	yes	no	no	no	no	Figure 14e
	1–2	Na-peroxide	yes	yes	yes	no	yes	no	no	Figure 14b
	1–2	4-acid	no	yes	yes	no	yes	NA	NA	Figure 14d
	1–2	aqua regia	yes	yes	yes	no	no	no	no	Figure 14a
Nb	<0.063	Na-peroxide	yes	no	no	yes	yes	yes	yes	Map 15
	<0.063	4-acid	no	no	no	yes	yes	no	NA	Map 17
	1–2	Na-peroxide	no	no	no	no	yes	yes	no	Map 16
	1–2	4-acid	no	yes	no	yes	no	no	NA	Map 18
Rb	<0.063	Na-peroxide	no	no	yes	no	no	yes	no	Map 10
	<0.063	4-acid	no	no	yes	no	no	no	no	Map 12
	1–2	Na-peroxide	yes	no	yes	yes	no	no	no	Map 11
	1–2	4-acid	no	no	yes	no	no	no	no	Map 13
Sn	<0.063	4-acid	no	no	yes	yes	no	no	no	Map 19
	1–2	4-acid	no	no	yes	yes	no	no	NA	Map 20
Ta	<0.063	Na-peroxide	no	no	yes	yes	yes	no	yes	Map 5
	<0.063	4-acid	no	no	no	yes	yes	no	NA	Map 7
	1–2	Na-peroxide	yes	yes	yes	yes	yes	no	no	Map 6
	1–2	4-acid	no	yes	yes	yes	yes	no	NA	Map 8
W	<0.063	4-acid	no	no	no	yes	no	no	NA	Map 21
	1–2	4-acid	no	yes	no	no	no	no	NA	Map 22
Zr	<0.063	4-acid	no	no	no	yes	no	no	NA	Map 14

Table 8. Lithium concentrations reported for other till geochemical studies and surveys compared to the concentrations reported in this study.

Location	Country	Source of information	Till size fraction	Analytical method	Highest Li value (ppm)	Pathfinder elements
Rampasaarat deposit	Finland	Ahtola et al., 2015	<0.064 mm	Na peroxide fusion/ICP-AES	5770	Li, Be
Kaustinen Li province	Finland	Kontoniemi, 2011	0.064–2 mm	Na peroxide fusion/ICP-AES	315	Li
Kaustinen Li province	Finland	Kontoniemi, 2012	0.06–0.5 mm	Na peroxide fusion/ICP-AES	1180	Li, Be
Kaustinen Li province	Finland	Kontoniemi, 2013	0.06–0.5 mm	Na peroxide fusion/ICP-AES	777	Li, Be
north-central Sweden	Sweden	Toverud, 1987	heavy minerals	AAS	109	Li
James Bay Region, Quebec	Canada	Li-FT Power, 2022	<0.063 mm	4-acid/ICP-MS	101	Li, Cs, Ta, Nb, Rb, Sn, Mn, Ga, P, W
central Newfoundland	Canada	Magyarosi, 2020	<0.180 mm	alkaline fusion/ ion selective electrode	948	F
SW New Brunswick	Canada	Rossiter, 2023	<0.063 mm	4-acid/ICP-MS	178	Li, Cs
East Side Road, SE Manitoba	Canada	Gauthier and Hodder, 2021	<0.063 mm	aqua regia/ICP-MS	42	Li, Cs
Fisher Branch, SE Manitoba	Canada	Hodder and Bater, 2016	<0.177 mm	4-acid/ICP-MS	51	Li, Cs
Brazil Lake, Nova Scotia	Canada	Palma et al., 1982	0.177–2.0 mm	multi-acid/AAS	228	Li, Sn, Ta
Brazil Lake, Nova Scotia	Canada	MacDonald et al., 1992	<0.063 mm	AAS	71	Li, Cs, Be
Brazil Lake, Nova Scotia	Canada	MacDonald et al., 1992	0.063–0.25 mm heavy minerals	AAS	334	Li, Cs, Be
Brazil Lake, Nova Scotia	Canada	Lundrigan, 2008	<0.063 mm	aqua regia/ICP-MS	76	Li
Brazil Lake, Nova Scotia	Canada	Lundrigan, 2008	1–2 mm	aqua regia/ICP-MS	777	Li
Brazil Lake, Nova Scotia	Canada	Lundrigan, 2008	<0.063 mm	4-acid/ICP-MS	73	Li
Brazil Lake, Nova Scotia	Canada	Lundrigan, 2008	1–2 mm	4-acid/ICP-MS	255	Li
Brazil Lake -this study	Canada	this study	<0.063 mm	aqua regia/ICP-MS	88	Li
Brazil Lake -this study	Canada	this study	1–2 mm	aqua regia/ICP-MS	86	Li
Brazil Lake -this study	Canada	this study	<0.063 mm	4-acid/ICP-MS	98	Li, Cs
Brazil Lake -this study	Canada	this study	1–2 mm	4-acid/ICP-MS	141	Li, Cs, Nb, Ta, W
Brazil Lake -this study	Canada	this study	<0.063 mm	Na peroxide fusion/ICP-MS	127	Li,Cs,
Brazil Lake -this study	Canada	this study	1–2 mm	Na peroxide fusion/ICP-MS	531	Li, Be, Cs, Rb, Ta

CONCLUSIONS AND RECOMMENDATIONS FOR EXPLORATION

Although drift prospecting for Li-pegmatites is not new, it has garnered a resurgence due to the demand for metals used in batteries. To date there has been no modern systematic guidelines developed for Li-drift prospecting in glaciated terrains. Presented here are the results for the first detailed investigation of three digestion methods (aqua-regia, 4-acid, and Na-peroxide fusion) for Li in till samples as well as a comparison of two size fractions (<0.063 and 1.0–2.0 mm).

- *Digestions:* Na-peroxide fusion is a "total" digestion for Li analyses and provides the most accurate results. A 4-acid digestion can provide similar results and is a method familiar to explorationists. Aqua-regia is only a partial digestion method for Li (on average 60% of the total concentration) but does provide results that have a strong systematic correlation with Na-peroxide fusion values as well as similar dispersal patterns on a regional scale.
- *Size fractions:* Commonly, the fine fraction (<0.063 mm) of till is analyzed for mineral exploration programs and regional-scale government surveys. The coarse fraction (1.0–2.0 mm) displays a larger contrast signal to background values than the fine fraction and provides a better defined dispersal anomaly when using Na-peroxide fusion. For regional exploration programs, the continued use of the fine fraction (<0.063 mm) is recommended. For property-scale and targeted exploration, Na-peroxide fusion using the 1.0–2.0 mm size fraction of till samples will provide the optimal results.
- *Sample size:* If only geochemical analysis is being conducted on till samples, a minimum of 500 g of till should be collected at each site to ensure that sufficient 1.0–2.0 mm and/or <0.063 mm fraction material can be recovered during sieving. Ideally, a kilogram (or more) of till (pebble-free) should be collected to allow for material to be archived in case reanalysis is required.
- *Sample spacing and orientation:* Given the small size of the pegmatites (up to 21 x 700 m for the larger North pegmatite) and the strong southward ice-flow directions recorded by landform and striation records, any resulting dispersal train will also be narrow, and till sampling should be along closely (250–500 m) spaced, parallel lines that are 1 to 2 km apart and oriented perpendicular to ice-flow.
- *Till facies:* Two till facies were observed in the study area and both are suitable for sampling for geochemistry. The first is a silty sand till that has moderate to high compaction, subhorizontal fissility with visible jointing, angular to subrounded local bedrock clasts, and numerous striated and faceted clasts. This is a 'subglacial traction till', a term that has superseded the older commonly used term, 'subglacial lodgement till'. A second till facies that often occurs in the study area as a thin (<2 m) horizon on the drumlin flanks is sandier, stonier, less indurated, less compact, contains well sorted lenses and layers of sand, and has more monolithic clast lithologies. This is a subglacial melt-out till.

What is the optimal digestion method and size fraction of till for Li exploration?

Two scenarios are discussed:

1) *Regional-scale grassroots exploration using new or legacy data sets:*

Based on the results presented here, for regional-scale exploration that may include other commodities, aqua regia digestion of the <0.063 mm fraction of till is sufficient. The strong correlation between the Li values from Na-peroxide fusion and aqua regia (R^2 = 0.86) highlights the similarity of distribution patterns, even though the aqua regia values are only about 60% of the total values reported by Na-peroxide fusion. Aqua regia is commonly used for base and precious metal exploration and its use in regional-scale surveys allows for the delineation of multiple commodities. Additionally, aqua regia is a routine digestion that is offered by most analytical laboratories and can be applied to the commonly used <0.063 mm size fraction.

Aqua regia has been widely used in exploration over the past 40 years and, as such, numerous historical data sets (government, exploration industry) of aqua regia results for the <0.063 mm fraction of till are available (e.g. Rossiter, 2023). These legacy data sets could be re-investigated/evaluated for Li and other pathfinder anomalies related to pegmatites. For routine analysis using aqua regia digestion, the collection of a 500 g bulk till sample is sufficient.

2) Property-specific targeting:

For property-specific Li targeting, a more informative, specialized, and costlier approach can be used. To effectively identify proximal dispersal of spodumene, analyses of the 1.0 to 2.0 mm till fraction using Na-peroxide fusion is recommended. Analysis of this coarse size fraction requires a pulverizing step prior to analysis. Of the six combinations of size fraction and analytical methods tested in this study, Na-peroxide fusion of the coarse (1–2 mm) fraction was the only method that identified a strong and obvious dispersal train of anomalous till derived from the Brazil Lake pegmatites (Fig. 14b, 18). In order to recover sufficient material for the analysis of the 1.0–2.0 mm fraction, a minimum of

500 g of raw till per sample must be collected. Table 6 provides a comparison of sample preparation and analytical costs for two size fractions and three analytical methods. These costs are the average of values reported by commercial labs in Canada at the time of writing. When deciding which size fraction and/or digestion to use, cost will inevitably also be a consideration.

What is the optimal sample spacing/density and survey orientation?

The answer to this can be somewhat complicated and varies depending on a number of factors. The small dimensions of a typical LCT pegmatite (e.g. 10 x 1000 m), and its orientation to the sequence of ice-flow events and their erosional vigour will significantly control the size and orientation of the resulting dispersed geochemical anomaly. At the Brazil Lake, the pegmatites are oriented almost parallel to ice-flow directions, which provides a point source diameter of ~21 m (the diameter of the larger North pegmatite). This scenario resulted in a small anomaly and, as such, a closely spaced sampling density would be required to identify its geochemical anomaly. For this case study, the location of the Brazil Lake pegmatites was known, but for greenfield explorers there is likely little, if any, information as to the size, shape, and orientation of the pegmatites. For areas similar to the Brazil Lake pegmatites example presented here, close (500 m) sample spacing along parallel lines (1–2 km apart) oriented perpendicular to the ice-flow direction would be recommended. An additional important consideration is the ice-flow directions relative to the orientation of structures and bedrock contacts that are more conducive to host pegmatites. Other considerations could include budgetary restrictions, property size, access, and existing data sets. There is no one option that is suitable to all situations.

ACKNOWLEDGEMENTS

The authors thank John Wightman, Greg Morris, and Cliff Stanley for access to the Brazil Lake property, field visits, and advice that guided the fieldwork. Adam Nissen, Saint Mary's University graduate student is thanked for field assistance in 2022. Mitch Maracle (NSDNRR summer student) is thanked for his assistance with fieldwork from 2020 to 2022. Alex Voinot (GSC) is thanked for his review of the report.

Two site visits were made to the Brazil Lake pegmatites with First Nation representatives in 2022. GSC and NSDNRR scientists met with Jeff Purdy (Councillor, Acadia First Nation), Greg Hart (NSPI Early Engagement Coordinator, Kwilmu'kw Mawklusuaqn Negotiation Office), and Patrick Butler (Mi'kmaq Energy & Mines Advisor, Kwilmu'kw Mawklusuaqn Negotiation Office) to explain the collaborative GSC-NSDNRR research at the site, the geology of the local lithium occurrence, answer questions, and address potential concerns about the impact of the fieldwork. We thank the Acadia First Nation for their interest in the research.

REFERENCES

Ahtola, T., Kuusela, J., Käpyaho, A., and Kontoniemi, O., 2015. Overview of lithium pegmatite exploration in the Kaustinen area in 2003–2012; Geological Survey of Finland, Report of Investigation 220, 28 p.

Barr, P.J.F. and Cullen, M.P., 2010. Technical report on the Brazil Lake lithium-bearing pegmatite property, Nova Scotia, Canada. https://goldfieldsns.com/locations/brazil-lake/.

Barros, R., Kaeter, D., Menuge, J.F., Fegan, T., and Harrop, J., 2022. Rare element enrichment in lithium pegmatite exomorphic halos and implications for exploration: evidence from the Leinster albite-spodumene pegmatite belt, southeast Ireland; Minerals, v. 12(8), 981. https://doi.org/10.3390/min12080981

Black, D.L., 2011. Lithium, Brazil Lake, Yarmouth County, Nova Scotia; Report on Diamond Drilling, Prospecting and Soil Gas Hydrocarbon Surveys, Brazil Lake Property, EL 05865 and EL 05866; Assessment Report ME 2011-032, 476 p.

Black, D.L., 2012. Report on prospecting, Brazil Lake property, EL 09083, EL09084, EL 09085; Assessment Report AR 2012-048, 476 p.

Brushett, D.M. and Tupper, J., 2021. Till geochemistry, indicator mineralogy, and surficial geology of the Brazil Lake pegmatite area, southwest Nova Scotia, Canada; *in* Geoscience and Mines Branch, Report of Activities 2020-2021, (ed.) D.R. MacDonald and E.W. MacDonald; Nova Scotia Department of Natural Resources and Renewables, Report ME 2021-002, p. 1–9.

Brushett, D.M., McClenaghan, M.B., and Paulen, R.C., 2022. Till geochemical data for the Brazil Lake Pegmatite area, Southwest Nova Scotia, Canada (NTS 21A/04, 20O/16 and 20P/13): till samples collected in 2020; Nova Scotia Department of Natural Resources and Renewables, Open File Report ME 2022-2.

Brushett, D.M., McClenaghan, M.B., Paulen, R.C., Beckett-Brown, C., Rice, J.M., Haji Egeh, A., and Nissen, A., 2023. Using till matrix geochemistry and LiDAR-based surficial geological mapping to understand glacial dispersal patterns associated with the Brazil Lake LCT pegmatites, southwest Nova Scotia, Canada; Poster session presented at the 49th Colloquium and Annual General Meeting of the Atlantic Geoscience Society, Truro, Nova Scotia.

Brushett, D.M., Kennedy, G.W., and MacMullen, C.C. in prep. Sediment thickness and bedrock topography maps of southwest Nova Scotia; Nova Scotia Department of Natural Resources and Renewables, Open File.

Černý, P., 1991. Rare element granite pegmatites. Part I. Anatomy and internal evolution of pegmatite deposits. Part II. Regional to global environments and petrogenesis; Geosciences Canada, v. 18, p. 49–67.

Černý, P. and Ercit, T.S., 2005. The classification of granitic pegmatites revisited; The Canadian Mineralogist, v. 43(6), p. 2005–2026. https://doi.org/10.2113/gscanmin.43.6.2005

Canadian Mining Journal, 2022. Champlain's first resource for Brazil Lake pegmatite in Nova Scotia; Canadian Mining Journal. https://www.canadianminingjournal.com/news/champlains-first-resource-for-brazil-lake-pegmatite-in-nova-scotia <Accessed May 5, 2022>

Chao, T.T. and Sanzolone, R.F., 1992. Decomposition techniques; Journal of Geochemical Exploration, v. 44, p. 65–106. https://doi.org/10.1016/0375-6742(92)90048-D

Charoy, B., Noronha, F., and Lima, A., 2001. Spodumene petalite eucryptite: mutual relationships and pattern of alteration in Li-rich aplite pegmatite dykes from northern Portugal; The Canadian Mineralogist, v. 39, p. 729–746.

Chudasama, B. and Sarala, P. 2022. Mineral prospectivity mapping of lithium-spodumene pegmatites in the Kaustinen region of Finland: implications for lithium exploration in Finland; Geological Survey of Finland, Open File Work Report 28/2022. https://tupa.gtk.fi/raportti/arkisto/28_2022.pdf

Critical Raw Materials, 2023. Facilitating the energy transition through lithium and rare earth exploration; Retrieved from https://www.innovationnewsnetwork.com/how-will-brazil-lake-lithium-project-power-energy-transition/33307/ <Accessed 2023/08/08>

Cullen, M., Harrington, M., and Elgert, L., 2022. NI 43-101 Technical report on the mineral resources estimate for the Brazil Lake project (lithium-bearing pegmatite deposit) Nova Scotia, Canada.

Culshaw, N. and Liesa, M., 1997. Alleghanian reactivation of the Acadian fold belt, Meguma Zone, southwest Nova Scotia; Canadian Journal of Earth Sciences, 34(6), p. 833–847. https://doi.org/10.1139/e17-068

Culshaw, N. and Reynolds, P., 1997. $^{40}Ar/^{39}Ar$ age of shear zones in the southwest Meguma Zone between Yarmouth and Meteghan, Nova Scotia; Canadian Journal of Earth Sciences, v. 34(6), p. 848–853. https://doi.org/10.1139/e17-069

de Souza, H., Seyfarth, A., Turner, N., and Woods, J., 2022. Lithium analyses of brines and minerals for exploration and resource definition; EXPLORE Newsletter for the Association of Applied Geochemists, no. 194. p. 1–13.

Evans, D.J.A., 2017. Till: A Glacial Process Sedimentology, First Edition; John Wiley & Sons Ltd. https://doi.org/10.1002/9781118652541

Finck, P.W. and Stea, R.R., 1995. The compositional development of tills overlying the South Mountain Batholith; Nova Scotia Department of Natural Resources, Mines and Minerals Branch, Paper 95-1, 52 p.

Gao, T.M., Fan, N., Chen, W., and Dai, T., 2023. Lithium extraction from hard rock lithium ores (spodumene, lepidolite, zinnwaldite, petalite): Technology, resources, environment and cost; China Geology, v. 6(1), p. 137–153. https://doi.org/10.31035/cg2022088

Gauthier, M.S. and Hodder, T.J., 2021. Till geochemistry from Manigotagan to Berens River, southeastern Manitoba (parts of NTS 62P1, 7, 8, 10, 15, 63A2, 7); Manitoba Geological Survey, Data Repository Item DRI2021006.

Girard, I., Klassen, R.A., and Laframboise, R., 2004. Sedimentology laboratory manual, Terrain Sciences Division; Geological Survey of Canada, Open File 4823, 137 p. https://doi:10.4095/216141

Grant, D.R., 1976. Reconnaissance of Early and Middle Wisconsinan deposits along the Yarmouth–Digby coast of Nova Scotia; Geological Survey of Canada, Report of Activities, Paper 76-1B, p. 363–369. https://doi.org/10.4095/104127

Grant, D.R., 1980. Quaternary stratigraphy of southwestern Nova Scotia: glacial events and sea level changes; Geological Association of Canada, Mineralogical Association of Canada, Field Trip Guidebook, Trip 9, 63 p.

Grant, D.R., 1987. Quaternary Geology of Nova Scotia and Newfoundland. INQUA Congress Field Excursion, A-3/C-3, 62 p.

Grant, D.R. and King, L.H., 1984. A stratigraphic framework for the Quaternary history of the Atlantic Provinces, Canada; *in* Quaternary Stratigraphy of Canada - A Canadian Contribution to IGCP Project 24, (ed.) R.J. Fulton; Geological Survey of Canada, Paper 84-10, p. 173–191.

Grenier, A., Connell-Madore, S., McClenaghan, M.B., Wygergangs, M., and Moore, C.S., 2015. Study of cleaning methods for electro-welded sieves to reduce/eliminate carry over contamination between till samples; Geological Survey of Canada, Open File 7769, 24 p. https://doi.org/10.4095/296314

Hibbard, J.P., van Staal, C.R., Rankin, D., and Williams, H., 2006. Lithotectonic map of the Appalachian orogen (north), Canada-United States of America; Geological Survey of Canada, Map 2041A, scale 1:1,500,000, 1 sheet.

Hodder, T.J. and Bater, C.W., 2016. Till-matrix (<177 μm) geochemistry analytical results from the Lynn Lake (parts of NTS 64C14, 64F3, 4), Southern Indian Lake (parts of NTS 64G8, 9), Churchill River (parts of NTS 64F14, 64K3, 6, 11) and Fisher Branch (NTS 62P) areas, Manitoba; Manitoba Geological Survey, Data Repository Item DRI2016004.

Keppie, J.D. and Krogh, T.E., 2000. 440 Ma igneous activity in the Meguma Terrane, Nova Scotia, Canada; part of the Appalachian overstep sequence?; American Journal of Science, v. 300(6), p. 528–538.

Kontak, D.J., 2004. Geology of the southern lobe of the Brazil Lake LCT-type pegmatite (NTS 21A/04), Yarmouth County, Nova Scotia; Nova Scotia Department of Natural Resources, Mineral Resources Branch, Report of Activities 2003, Report 2004-1, p. 41–68.

Kontak, D.J., 2006. Nature and origin of an LCT-suite pegmatite with late-stage sodium enrichment, Brazil Lake, Yarmouth County, Nova Scotia. I. Geological setting and petrology; The Canadian Mineralogist, v. 44(3), p. 563–598. https://doi.org/10.2113/gscanmin.44.3.563

Kontak, D.J. and Kyser, T.K., 2009. Nature and origin of an LCT-suite pegmatite with late-stage sodium enrichment, Brazil Lake, Yarmouth County, Nova Scotia. II. Implications of stable isotopes ($\delta^{18}O$, δD) for magma source, internal crystallization and nature of sodium metasomatism; The Canadian Mineralogist, v. 47(4), p. 745–764. https://doi.org/10.3749/canmin.47.4.745

Kontak, D.J., Creaser, R.A., Heaman, L.M., and Archibald, D.A., 2005. U-Pb tantalite, Re-Os molybdenite, and $^{40}Ar/^{39}Ar$ muscovite dating of the Brazil Lake pegmatite, Nova Scotia: a possible shear-zone related origin for an LCT-type pegmatite; Atlantic Geology, v. 41(1), p. 17–29.

Kontoniemi, O., 2011. Kaustisen seudun litium-varannot-hankkeen (KaLi) tukimukset vuosina 2010–2011; Geologian tutkimuskeskus, Geological Survey of Finland, unpublished report 35/2011. 18 p. (in Finnish).

Kontoniemi, O., 2012. Kaustisen alueen Li-potentiaali – van-hojen moreeninäytteiden uudelleenanalysointi; liitekarttaa Geologian tutkimuskeskus, Geological Survey of Finland, unpublished report 68/2012. 12 p. (in Finnish).

Kontoniemi, O., 2013. Kaustisen alueen Li-potentiaali – van-hojen moreeninäytteiden uudelleenanalysointi, vaihe 2; Geologian tutkimuskeskus, Geological Survey of Finland, unpublished report 52/2013. (in Finnish).

Li-FT Power, 2022. Li-FT Power provides exploration results for 2022 Rupert project exploration program; Junior Mining Network. Accessed Oct. 23, 2023. https://www.juniorminingnetwork.com/junior-miner-news/press-releases/3217-cse/lift/130848-li-ft-provides-exploration-results-from-2022-rupert-project-exploration-program.html

London, D. and Burt, D.M., 1982. Alteration of spodumene, montebrasite and lithiophilite in pegmatites of the White Picacho District, Arizona; American Mineralogist, v. 67, p. 97–113.

Lundrigan, A., 2008. Glacial stratigraphy and till geochemical dispersion controls associated with the Brazil Lake pegmatite, southwestern Nova Scotia; M.Sc. Thesis, Acadia University, Wolfville, Nova Scotia, 309 p.

MacDonald, M.A., Boner, F.J., and Lombard, P.A., 1992. Multimedia detailed geochemical study of the Brazil Lake pegmatites (NTS 20P/13), Yarmouth County, Nova Scotia; Nova Scotia Department of Natural Resources, Open File Report 92-016, 159 p.

Marsden, J. and House, I., 2006. The chemistry of gold extraction (second edition); Society for Mining, Metallurgy, and Exploration, p. 651.

Magyarosi, Z., 2020. Rare element enriched pegmatites in central Newfoundland; *in* Current Research 2020; Newfoundland and Labrador Department of Natural Resources, Geological Survey, Report 201, p. 121–143.

McClenaghan, M.B. and Paulen, R.C., 2018. Mineral exploration in glaciated terrain, Chapter 20; *in* Past Glacial Environments (Sediments, Forms and Techniques): A new and revised edition; Elsevier, p. 689–751.

McClenaghan, M.B., Spirito, W.A., Plouffe, A., McMartin, I., Campbell, J.E., Paulen, R.C., Garrett, R.G., Hall, G.E.M., Pelchat, P., and Gauthier, M.S., 2020. Geological Survey of Canada till-sampling and analytical protocols: from field to archive, 2020 update; Geological Survey of Canada, Open File 8591, 73 p. https://doi.org/10.4095/326162

McClenaghan, M.B., Brushett, D.M., Paulen, R.C., Beckett-Brown, C.E., Rice, J.M., Haji Egeh, A., and Nissen, A., 2023a. Critical metal indicator mineral studies of till samples collected around the Brazil Lake LCT pegmatite, southwest Nova Scotia; Geological Survey of Canada, Open File 8960, 12 p. https://doi.org/10.4095/331537

McClenaghan, M.B., Brushett, D.M., Beckett-Brown, C.E., Paulen, R.C., Rice, J.M., Haji Egeh, A., and Nissen, A., 2023b. Indicator mineral studies at the Brazil Lake LCT pegmatites, southwest Nova Scotia; Geological Survey of Canada, Scientific Presentation 157. https://doi.org/10.4095/331686

McClenaghan, M.B., Paulen, R.C., Smith, I.R., Rice, J.M., Plouffe, A., McMartin, I., Campbell, J.E., Lehtonen, M., Parsasadr, M., and Beckett-Brown, C.E., 2023c. Review of till geochemistry and indicator mineral methods for mineral exploration in glaciated terrain; Geochemistry: Exploration, Environment, Analysis, v. 23. https://doi.org/10.1144/geochem2023-013

Nikkarinen, M. and Björklund, A., 1975. The use of till in spodumene exploration; *in* Conceptual Models in Exploration Geochemistry: Norden 1975, (ed.) L.K. Kauranne; Journal of Geochemical Exploration, v. 5 p. 212–214. https://doi.org/10.1016/0375-6742(76)90048-0.

Palma, V.V., Sinclair, P.E., Hutchinson, H.E., and Kohlsmith, R.L., 1982. Report on geological mapping, till and rock geochemical surveys, and magnetic and VLF-EM surveys at Brazil Lake, Yarmouth County, Nova Scotia; Shell Canada Resources Ltd.; Nova Scotia Department of Natural Resources, Assessment Report 434310.

Plouffe, A., McClenaghan, M.B., Paulen, R.C., McMartin, I., Campbell, J.E., and Spirito, W.A., 2013. Processing of glacial sediments for the recovery of indicator minerals: protocols used at the Geological Survey of Canada; Geochemistry: Exploration, Environment, Analysis, v. 13, p. 303–316. https://doi.org/10.1144/geochem2011-109.

Rasilainen, K., Eilu, P., Ahtola, T., Halkoaho, T., Kärkkäinen, N., Kuusela, J., Lintinen, P., and Törmänen, T., 2018. Quantitative assessment of undiscovered resources in lithium-caesium-tantalum pegmatite-hosted deposits in Finland; Geological Survey of Finland, Bulletin 406. http://doi.org/10.30440/bt406.

Rogers, P.J., MacDonald, M.A., and Rigby, D.W., 1985. Regional lake sediment survey of the Meguma Zone, southern Nova Scotia; new analytical data; Nova Scotia Department of Mines and Energy, Open File Report 605, 65 p.

Rogers, P.J., Chatterjee, A.K., and Aucott, J.W., 1990. Metallogenic domains and their reflection in regional lake sediment surveys from the Meguma Zone, southern Nova Scotia, Canada; Journal of Geochemical Exploration, v. 39, p. 153–174. https://doi.org/10.1016/0375-6742(90)90072-I.

Rossiter, S.L.E., 2023. Lithium and cesium anomalies in till in southwestern New Brunswick; New Brunswick Department of Natural Resources and Energy Development, Open File 2023-3.

Sarapää, O., Kärkkäinen, N., Ahtola, T., and Al-Ani, T., 2015. High-tech metals in Finland; Chapter 9.2 *in* Mineral Deposits of Finland, (ed.) W.D. Maier, R. Lahtinen, and H. O'Brien; p. 613–632. https://doi.org/10.1016/B978-0-12-410438-9.00023-6

Schultz, R.W., 1971. Mineral exploration practice in Ireland; Transactions of the Institution of Mining and Metallurgy, Section B: Applied Earth Science, v. 80, p. 238–258.

Shaw, J., Piper, D.J.W., Fader, G.B.J., King, E.L., Todd, B., Bell, T., Batterson, M.J., and Liverman, D.G.E., 2006. A conceptual model of the deglaciation of Atlantic Canada; Quaternary Science Reviews, v. 25(17-18), p. 2059–2081. https://doi.org/10.1016/j.quascirev.2006.03.002

Smith, C.G., 2019. Geochemical and mineralogical dispersal in till from the East Kemptville Sn-An-Cu-Ag deposit, southwest Nova Scotia; B.Sc. thesis, Acadia University, Wolfville, Nova Scotia, 128 p.

Spirito, W.A, McClenaghan, M.B., Plouffe, A., McMartin, I., Campbell, J.E., Paulen, R.C., Garrett, R.G., and Hall, G.E.M., 2011. Till sampling and analytical protocols for GEM Projects: from field to archive; Geological Survey of Canada, Open File 6850, 83 p. https://doi.org/10.4095/300281

Stea, R.R., 2004. The Appalachian Glacier Complex in Maritime Canada; *in* Developments in Quaternary Sciences, Volume 2, Part B, p. 213–232. https://doi.org/10.1016/S1571-0866(04)80199-4

Stea, R.R. and Grant, D.R., 1982. Pleistocene geology and till geochemistry of southwestern Nova Scotia (sheets 7 and 8); Nova Scotia Department of Mines and Energy, Map 82-10, scale 1:100 000.

Stea, R.R. and Finck, P.W., 2001. An evolutionary model of glacial dispersal and till genesis in Maritime Canada; *in* Drift Exploration in Glaciated Terrain, (ed.) M.B. McClenaghan, P.T. Bobrowsky, G.E.M. Hall, and S.J. Cook; Geological Society of London, Special Publication 185, p. 237–265. https://doi.org/10.1144/GSL.SP.2001.185.01.11

Stea, R.R., Fader, G.B.J., and Boyd, R., 1992. Quaternary seismic stratigraphy of the inner shelf region, Eastern Shore, Nova Scotia; *in* Current Research, Part D. Geological Survey of Canada, Paper 92-1D, p. 179–188. https://doi.org/10.4095/133955

Stea, R.R., Seaman, A.A., Pronk, T., Parkhill, M.A., Allard, S., and Utting, D., 2011. The Appalachian Glacier Complex in Maritime Canada; *in* Developments in Quaternary Sciences, v. 15, p. 631–659. https://doi.org/10.1016/S1571-0866(04)80199-4

Steiner, B.M., 2019. Tools and Workflows for Grassroots Li-Cs-Ta (LCT) Pegmatite Exploration; Minerals, v. 9, p. 1–23. https://doi.org/10.3390/min9080499

Steiger, R., 1977. Prospecting for lithium and tungsten in Ireland; *in* Prospecting in Areas of Glaciated Terrain 1977; Canadian Institution of Mining and Metallurgy, p. 14–24.

Stokes, C.R. and Clark, C.D., 2002. Are long subglacial bedforms indicative of fast ice flow?; Boreas, v. 31, p. 239–249. https://doi.org/10.1111/j.1502-3885.2002.tb01070.x

Taylor, F.C., 1967. Reconnaissance geology of the Shelburne map-area, Queen's, Shelburne, and Yarmouth counties, Nova Scotia; Geological Survey of Canada, Memoir 349, 83 p.

Toverud, Ö., 1987. Vastani-Jarkvissle Sn-Li occurrence found by regional grid sampling of heavy-mineral till concentrates in northern central Sweden; Journal of Geochemical Exploration, v. 28, p. 369–383. https://doi.org/10.1016/0375-6742(87)90058-6

White, C.E., 2010. Stratigraphy of the lower Paleozoic Goldenville and Halifax groups in southwestern Nova Scotia; Atlantic Geology, v. 46, p. 136–154. https://doi:10.4138/atlgeol.2010.008

White, C.E. and Barr, S.M., 2017. Stratigraphy and depositional setting of the Silurian–Devonian Rockville Notch Group, Meguma terrane, Nova Scotia, Canada; Atlantic Geology, v. 53, p. 337–365. https://doi:10.4138/atlgeol.2017.015

White, C.E., Palacios, T., Jensen, S., and Barr, S.M., 2012. Cambrian–Ordovician acritarchs in the Meguma terrane, Nova Scotia, Canada: Resolution of early Paleozoic stratigraphy and implications for paleogeography; Geological Society of America, Bulletin 124(11-12), p. 1773–1792. https://doi.org/10.1130/B30638.1

White, C.E., Barr, S.M., and Linnemann, U., 2018. U–Pb (zircon) ages and provenance of the White Rock Formation of the Rockville Notch Group, Meguma terrane, Nova Scotia, Canada: evidence for the "Sardian gap" and West African origin; Canadian Journal of Earth Sciences, v. 55(6), p. 589–603. https://doi.org/10.1139/cjes-2017-0196

Wightman, J.F., 2018. Report on work conducted under funding provided through NSMIP PG-2017-17: Assessment report on sampling, Deerfield, Yarmouth County, N.S., Brazil Lake Property, EL 50904; Nova Scotia Department of Natural Resources, ME-1043173, 144 p.

Wightman, J.F., 2020. Report on work conducted under funding provided through NSMIP PG-2017-17, Assessment report on soil sampling, Deerfield, Yarmouth County, N.S.; Nova Scotia Mineral Incentive Program Prospector Grant 2017-17, Open File Report ME 2020-013, 303 p.

Williams, H., Kennedy, M.J., and Neale, E.R.W., 1974. The northeastward termination of the Appalachian orogen; The Ocean Basins and Margins: The North Atlantic, v. 2, p. 79–123.

Yu, Z., Robinson, P., and McGoldrick, P., 2007. An evaluation of methods for the chemical decomposition of geological materials for trace element determination using ICP-MS; Geostandards Newsletter, v. 25, p. 199–217.